UNIVERSITATEA POLITEHNICA DIN BUCUREȘTI
Facultatea de Inginerie Industrială și Robotică
Departamentul de Rezistența Materialelor

SUMMARY
PhD THESIS

Studiul teoretic și experimental privind tranziția palei anticuplu a elicopterului IAR330 către o configurație constructivă compozită

Experimental and theoretical study of the transition towards a composite configuration for the IAR330 tail rotor blade

Author: ing. Andrei-Daniel VOICU

PhD Supervisor: Prof. dr. ing. Anton HADĂR

Bucharest
2022

Keywords: fiber reinforced composite materials, hand lay-up composite manufacturing, additive manufacturing, fused deposition modeling, honeycomb core, tail rotor blade, tensile test, compression test, three point bending test, finite element analysis, finite element model validation, aerodynamic wind tunnel, aerodynamic loads.

Table of contents

INTRODUCTION

CURRENT TOPICS RELATED TO THE THESIS

In the evolutionary context of mankind, technological progress has been the main propulsion engine for economic and industrial development of the world. This progress was closely related, especially in the proximity of the industrial revolution in the 18th and 19th centuries, to the level of knowledge related to the mechanical properties of materials, on the one hand, and the establishment of mathematical relations regarding the strength of materials, on the other hand. The first barriers in this field were overcomed by renowned figures in mathematics, such as Robert Hooke, Euler, Coulomb and Navier [1], who gradually paved the way to the establishment of the Polytechnic Institute of Paris in the 18th century, where many generations of prestigious engineers and mathematicians were formed.

Composite materials represent a distinct category of materials, which were used even by ancient civilizations, such as the Egyptians, by combining mud with straws to obtain a structure that combines the best properties of the constituent materials. However, their development and more in-depth research was carried out at the beginning of the 19th century, with the emergence of plastic materials, such as polyester, polystyrene, vinyl, etc., representing synthetic materials with superior properties as compared to resins obtained from nature. The use of glass fiber to reinforce the matrix made of a synthetic resin in 1935 by Owens Corning, marked the beginning of the development of fiber reinforced plastic composite materials [2]. Since that time, composite materials have been the subject of intense studies, being used together with cellular materials, such as polyurethane foams or honeycomb structures, to form sandwich structures, which offer superior structural properties.

The main current applications of composite materials are met in the automotive, aerospace or naval industries, due to the high resistance they possess to operational stresses, while offering, at the same time, a considerable decrease in the total mass of the structures.

Additive manufacturing is a domain under development, which is based on the creation of components with a complex geometry, that could not have been realized by classical manufacturing means. The diversity of emerging technologies in this field allows various operations, such as the realization of rapid prototyping for domestic applications through thermoplastic extrusion, commercially called "3D printing", but also the creation of essential components, such as the fuel injectors from the GE9X turbojet engines of Boeing 777X commercial aircraft [3], a fact which confirms the confidence given to these manufacturing technologies by the aerospace industry.

Each additive manufacturing method has its own advantages and disadvantages, especially in what concerns the manufacturing time, the variaty of materials that can be used, the overall strength of the final product, the need to integrate temporary supports at the time of manufacture and the final degree of exterior finish.

Honeycomb structures are a type of modern cellular material designed to meet the specific strength and mass requirements demanded by the beneficiary. Specialized software programs for additive manufacturing have dedicated modules in their composition, containing libraries of unit cell elements. Thus, by means of topological optimization and intuitive artificial intelligence, in the near future it will be possible to manufacture structures with extremely complex geometries, practically impossible to achieve today.

The actuality of the topic consists in combining 3D printed composite structures, with the advantages of classic fiber reinforced composite materials, to develop an anti-torque rotor blade for the IAR330 helicopter, with superior performances compared to the blade made of aluminum alloy.

IMPORTANCE OF THE SUBJECT

Increasing the performance of the IAR330 helicopters, by modernizing certain components, represents an important objective for the Romanian Air Force, in the current geopolitical context. Multirole helicopters require the use of modern manufacturing technologies, which incorporate high-performance materials in terms of resistance to aerodynamic demands.

In recent years, composite materials have become the preferred choice for component manufacturers in the aerospace industry, as their resistance to environmental conditions and demands during aircraft flight has been demonstrated, both theoretically and practically. Military helicopters have to endure environmental conditions and much more varied demands compared to civil aircraft, thus resulting in the need to manufacture them from sustainable materials, with a practically unlimited technical resource.

Due to the specific take-off mode of the helicopter, it must lift all its mass to detach from the ground, hence the desire to reduce it. Thus, according to Airbus, the helicopters have experienced a very high degree of integration of composite materials, being used in a proportion of 80% for the structure of the Airbus Tiger helicopter and 90% for the NH90 helicopter model. In terms of transportation aircraft, about a quarter of the structure of the A380 model is made from composite materials [4]. Thus, the increasing adoption of composite materials as main elements in aircraft structure can be observed.

Consequently, mass reduction is a very important aspect in helicopter manufacturing. In addition to the contribution of composite materials in this regard, the additive manufacturing of the honeycomb structure allows the most efficient use of space in the interior of structures, so as to achieve the best possible ratio between stiffness and the total mass of the manufactured components. The use of fiber-reinforced laminated composite materials together with 3D printed thermoplastic paves the way for hybrid manufactured structures, a subject of interest in aerospace applications.

The use of cellular elements with a satisfactory geometry, such as cubic cells, or octahedron, gyroid or diamond type elements, gives the structure increased stress resistance during flight. Starting from a cellular element with an established geometry, by means of an optimization software, its size can be varied in certain areas of the interior space intended for the honeycomb structure, in case of more exigent material demands.

Experimental validation represents the final stage in the practical development of the composite anti-torque blade concept, achieved through practical test methods, such as the subsonic wind tunnel or by applying a bending force on the free end of the blade. The validation of such a model is of particular importance, because the development method can be adapted to any similar structure, not only from the aerospace field, thus contributing to the progressive evolution of aviation structures towards a new generation of high-performance aircraft.

1. CURRENT RESEARCH STATUS

1.1 Composite materials. Clasification, evolution and main characteristics

Composite materials represent a relatively modern class of materials, made by combining two or more components, which have different physical and chemical characteristics, in a material with superior characteristics compared to each individual constituent material. Their main characteristic is related to the orthotropic character, in that they have customizable properties according to the user's requirements, so that, through the appropriate positioning of the constituents, the final material has the best resistance properties in the main direction of stress.

Aircraft blades represent structures of particular importance in their construction, having a role in the propulsion and directional control of aircraft, on whose good functioning depends the ability to ensure flight safety. These are active aerodynamic components, being responsible for generating the thrust force used for propulsion and directional control of aircraft. The manufacturing material has seen a constant evolution, being directly related to the general aircraft level of performance.

The most common categories of materials used in the construction of aerospace structures, as well as their main characteristics are [5]:

- *metals* – represents the classic material solution, used especially before the introduction of composite materials in aircraft construction; they are characterized by a low resistance with increasing operating temperature and a relatively high mass, compared to modern materials; are still used today by previous aircraft generations still in active service, but they are no longer used to manufacture propellants;
- *polymers* – are materials made of repeating chains of molecules; they can be of synthetic origin (plastic materials) or natural (rubber, wood) and are especially resistant to low temperatures, but have a lower cost and density compared to metals; they are not generally used as structural elements;
- *ceramics* – they are superior to metals and polymeric materials in terms of resistance to high temperatures and thermal expansion, but they are more fragile (brittle); the aerospace industry uses alumina ceramic-based materials, polycrystalline materials (ceramic glass) or composite materials with a ceramic matrix as the main materials;
- *composite materials* – represents the most frequently used material category within aeronautical structures, due to their superior properties compared to the other categories of materials, as well as due to the possibility of customizing the properties of the final material, by choosing the optimal constituents, arranged with the right orientation; proof of their importance results from the growing interest in their use in the aircraft manufacturing and also, in other aerospace structures.

Figure 1.1 shows the main materials used in the composition of two commercial aircraft, recently developed by the most important aircraft manufacturers worldwide. The transition to this category of materials is carried out in taking into account the need to obtain increased performance, based on the highest strength-to-mass ratio of the components. As can be seen in these figures, composite materials already comprise a large proportion of aircraft structures, being fully adopted as the constructive and manufacturing challenges are overcomed with the help of technological advancement.

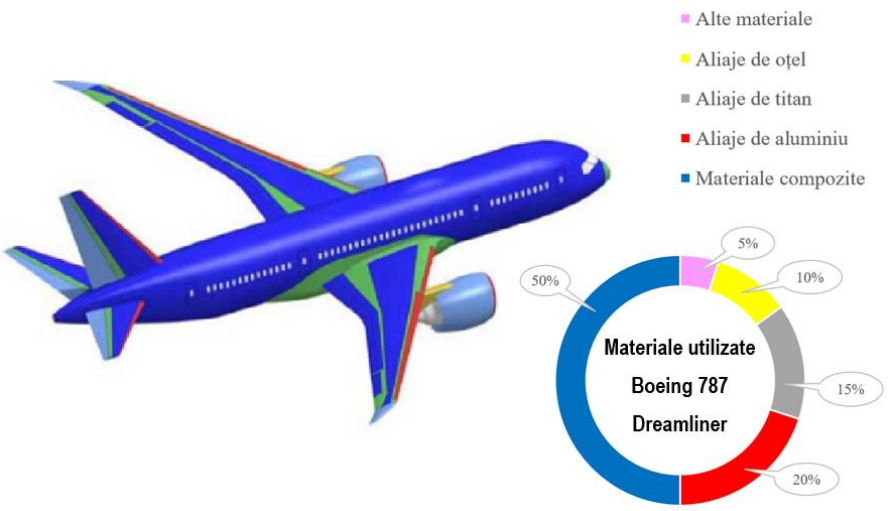

Fig. 1.1 Materials used to manufacture the Boeing 787 Dreamliner [6]

Although the use of composites presents numerous advantages, there are also numerous challenges that must be overcome, these being generated by their anisotropic and sometimes inhomogeneous character, requiring the development of manufacturing processes that can be adapted according to the characteristics of the material. Also, when subjecting them to different types of loads, they have a complex behavior, difficult to predict, requiring the use of equally complex study tools.

The finite elements analysis programs (such as Abaqus, Solidworks, Ansys, Catia, etc.) and the analysis methods within them, allow the realization of approximate numerical simulations, when appropriate initial data is introduced. Thus, structural components can be modeled, analyzed and optimized in a much shorter time frame, with experimental validation being carried out using test facilities that reproduce as accurately as possible the mechanical behaviour met during normal functioning conditions.

The use of modern computational systems in all stages of design, manufacture and analysis of these materials, facilitates obtaining accurate and easy to display graphically results, to met the performance requirements in this field.

The main structural components of an aircraft fully or partially made of composite materials are the following [7]:

- aircraft fuselage;
- flight control surfaces (rudder, elevator);
- propellar of turboprop engines or the fan section of turbofan engines;
- aircraft wing and its structure, in the case of modern aircraft;
- interior components, such as the floor of the aircraft, certain parts of the passenger seats, etc.

Composite materials represent a distinct class of materials, by their nature and manufacturing method, and can be classified as follows [8] :

- *fibrous composite materials* – based on materials manufactured in the form of fibers, inserted inside the matrix that joins the structure into a unitary material; the final product is an anisotropic material, but which can offer superior performances compared to other materials, by using constituents with a higher strength;
- *laminated composite materials* – obtained by overlapping different layers of materials; the layers can be manufactured from fabrics positioned at different orientations, depending on the direction of action of the external forces, being joined in a single solid structure, by means of a polymer adhesive;

- special composite materials (reinforced with particles) – they are manufactured by inserting material particles into another material, called the matrix; they are rarely used in the aerospace industry, the most common example of such a material being cement.

Fibers are characterized by a much higher resistance to tensile stress than the material in massive form, due to the purity of the material and its internal structure. Depending on the ratio between length *l* and diameter *d*, the fibers can be continuous (l/d > 1000) or discontinuous (l/d < 1000). The materials with the highest applicability in the aeronautical industry in this form are glass, carbon and Kevlar fibers.

Fiber orientation is an important characteristic that influences the tensile strength of a composite material. In the case of carbon fiber, its strength ranges from values close similar to that of glass fibers and can reach values similar to titanium, depending mainly on the orientation of the fibers in relation to the direction of the applied forces. The appropriate choice of this orientation is important to achieve an efficient structure. Therefore, in composite structure maintenance that require laminate skin replacement, it is necessary that the new CFRP is made of the same material and has the same fiber orientation as that of the damaged material.

The matrix is the second important element in the composition of composite materials, that has the role of uniting the fibers into a unitary solid material, protecting them at the same time, by transferring the stress and redistributing the efforts when the fibers break. This ensures an increased stiffness of the composite material and, at the same time, a reduced mass.

Laminated composite materials consist of two or more materials, joined by means of an adhesive. A separate category is represented by fiber-reinforced laminated composite materials, due to their applicability in fabricating propulsive elements. They are manufactured from a sequence of superimposed laminas, so that the fibers of a lamina are parallel, and the layer is characterized by a certain orientation, with the aim of obtaining the highest resistance possible.

Sandwich structures represent a constructive solution used on a large scale, due to their many advantages, compared to other types of materials. Among them can be listed: low mass, high stability, etc.

A sandwich-type structure is made, in the simplest version, from two thin parallel shells, glued to a central core, which has a low mass. This central element supports the two parallel faces and is characterized by high resistance to shear and compression stresses. The manufacturing process is most commonly done by maturing in autoclaves or using a press. Honeycomb structures or foams with special properties are generally used for the central structure. The central honeycomb structure is used in the following aircraft structural elements: wing, spoilers, ailerons, nacelles, cabin floor, etc.

Sandwich structures have the advantage of high bending strength, whilst having, at the same time, a reduced mass compared to aluminum structures or laminated composite materials. By increasing the thickness of the central honeycomb structure, the rigidity of the structure can be increased. Therefore, the structure does not require additional external resistance elements, such as bars or resistance frames.

The materials used to make the outer faces are aluminum, glass fiber, carbon fiber or Kevlar. Carbon fiber is not used in the case of a central honeycomb structure, because, in combination with other metals, it would lead to their corrosion. In general, these covers are relatively thin, sometimes made of three or four layers, and have low impact resistance.

The fibers are the reinforcing components in composite materials, which provide rigidity and prevent the propagation of cracks. Thin fibers can have very high strength, provided there is good cohesion with the matrix of the composite material. Depending on the length of the fibers incorporated in the composite material, they can be classified as continuous fibers or short fibers. Continuous fibers are most often used to make fiber-reinforced laminate composites, while short fibers are usually dispersed in the composite matrix.

The main materials used to make fibers, with the aim of using them in composite materials, are: carbon (C), bor, (B), aluminum (Al) și silicon (Si). They have low atomic number

and are preferred in such applications due to strong interatomic bonds. Their processing in the form of fibers can be made entirely from the same material or in the form of various compounds (SiO_2, SIC, Al_2O_3 etc.). Their failure mode differs depending on the molecular nature of the material.

The matrix used in the composition of a composite material represents that structural element that fulfills the following purposes:

- receives/transfers requests from/to fibers;
- separates the fibers to prevent multiple fibers from breaking, if some of them fail;
- protects the fibers from environmental factors and integrates them inside the composite material.

The properties of a composite material that incorporates a polymer matrix are: the compressive strength in the longitudinal axis, the tensile strength in the transverse plane and the interlaminar shear strength.

To fulfill the role of a matrix within a composite material used in the aerospace industry, the polymer must have good chemical resistance, when it comes into contact with special liquids, such as hydraulic fluid, fuel or paint stripper. A very important aspect in manufacturing composite materials is that the integration of the polymer matrix in the final product does not damage the fibers used for reinforcement, nor does it change their position/orientation.

Thermosetting polymers are those polymers that harden irreversibly in certain conditions of temperature and pressure, through the ripening process of a viscous polymer liquid or resin. The polymer is found in a malleable/liquid form so that it can be molded/cast into the final shape. The main examples of thermosetting polymers are:

- polyester resin – laminated composite materials;
- polyurethane resin – adhesives, insulating foams, protective layers;
- epoxy resin – adhesives, plastic materials reinforced with fibers;
- polyamide resin – aerospace composite structures, electronic boards;
- silicone resin – polymeric composite materials;
- vinylester resin – structural repairs, lamina adhesion.

Thermoplastic polymers are materials that are malleable at high temperatures and solidify when cooled. They are used to make various structural components, through injection, extrusion or compression processes. Compared to heat-resistant polymers, which solidify irreversibly, by heating above a certain temperature threshold, they return to the malleable state where they can be modified/processed according to requirements [9].

Epoxy resins – represent the most used heat-resistant type of resin in aerospace structures. This class of compounds consists of two or more epoxy groups per molecule, has very good chemical and mechanical properties, and exhibits good adhesion to most fiber types.

The final properties of a matrix made of epoxy resin are dependent on the following main aspects:

- choosing the appropriate epoxy resin;
- choosing the appropriate maturing (hardening) agent;
- the addition of specific additives.

Thermoplastic resins used in the aerospace industry are more expensive to produce than thermosetting resins, due to the need to ensure operation at high temperatures and pressures. Recent development and improvements in thermosetting resins have begun to overshadow the advantage of thermoplastic resins in being more resistant, taking over some of the tasks previously held by them, in terms of making certain structural elements. However, thermoplastic polymers will continue to be used in important structural elements, where impact resistance and resistance to operational stress are an essential condition.

1.2 Methods of manufacturing composite blades and classification of frequent damage types

There are many methods used to manufacture composite materials for the aeronautical industry. The manufacturing choice for a specific component depends on: the materials used, the geometry (shape) of the part and how its functional characteristics.

The manufacturing process involves, in most cases, the use of a mold or a device to give the processed material the desired shape. This step is carried out before and during the ripening process. An embodiment of this process consists of using a piston type mold. To obtain a high quality laminate it is important to know the amount of reinforcing fibers needed to fill the mold.

One way of manufacturing composite materials is by infusing a resin inside a mold [10]. A propeller made through this method must have the appropriate characteristics in all three of its dimensions.

Another variant of the manufacturing process involves the use of a vacuum pump, to suck the resin from a tank, in order to fill the mold [11]. Dry fibers, regardless of their type (unidirectional or woven) are placed in a sealed membrane inside a mold.

This method provides satisfactory results, being viable for large components, but it has a higher degree of complexity compared to other manufacturing techniques. The density of the resin used plays an important role in the manufacturing process, as there is a need to use low-density resins, which leads to weaker mechanical properties than in the case of dense resins.

A more simplistic but effective method of making composite blades is by manually placing the laminae (hand lay-up) in a predetermined sequence, based on the fabric orientation. The positioning of each individual lamina is followed by impregnating it with resin and smoothing it using a roller device. Curing takes place at room temperature or 70-100°C for epoxy resin.

The main types of damage encountered by composite materials are those that occur during normal operation or during the manufacturing process. Similar to conventional metals used for various resistance structures, composite materials, having several constituents and a pronounced anisotropic character, are not immune to such defects or damage.

In the manufacturing process there are numerous factors that influence the quality of the final material, and among the defects that appear during this process, can be found [12]:

- unevenly positioned lamellas;
- unevenly distributed resin;
- missing or cut fibers;
- partially solidified resin;
- pores, air inclusions or impurities inside the material;
- impact with foreign bodies during manufacturing;
- factors of the manufacturing environment, external pollutants;
- veiling of fibers or fabric, etc.

Also, in the normal functioning conditions, there are numerous factors that can lead to material damage, depending on the operating conditions. Some of these may be:

- resin rupture;
- delamination;
- ungluing;
- breaking or tearing of fibers;
- micro-veiling;
- external loads applied during normal usage;
- loads arising during assembly/disassembly;
- vibrations during transportation;
- impact with foreign bodies, etc.

Matrix cracking is the type of damage that occurs between two or more layers of the composite material, positioned parallel to the fabric fibers. As a rule, this type of damage does not represent an immediate problem for the structural integrity of the composite material, being only a starting point for other modes of failure of composite materials [13].

Fiber breakage is a damage that leads to the reduction of both the modulus of elasticity of the material and its load-bearing capacity. The initiation of fiber breakage has a more pronounced effect on the tension at which the veiling of the material occurs than the reduction of its stiffness. Thus, for safety reasons, it is important to investigate the bearing capacity of the composite material when this type of damage is observed.

1.3 Existing structures and their applicability for manufacturing composite tail rotor blades

The anti-torque rotor blade is one of the components of the helicopter subjected to continuous stress during its operation, the degree of stress being influenced by many aspects, such as:

- environmental factors (temperature, atmospheric pressure, humidity);
- impact/interference with various foreign bodies;
- modification of the aerodynamic characteristics along the length of the blade (pressure distribution, air flow around the blade), due to gusts of wind or due to changes of the blade incidence;
- changing the incidence of the blade.

Due to its geometrical characteristics, the anti-torque blade of the helicopter can be modeled in one of the following three ways: three-dimensional geometric model - made with the finite element method, two-dimensional geometric model - based on the cross-section of the blade and its length or one-dimensional geometric model - a solid beam model. There are studies on the optimal way of modeling the geometry of the anti-torque blade, so that the results obtained from the numerical analyzes are as close as possible to the experimental data. In principle, the three-dimensional model provides the most accurate results, but the calculation time is much higher, compared to the other two variants. On the other hand, realizing the geometry as a simplified two-dimensional or one-dimensional model has the advantage of a much shorter calculation time, and by using programs specially designed for this purpose, the final results can be close enough to the real ones.

A. *Exterior loads applied on the blade* – The main forces acting on the anti-torque blade of the IAR330 helicopter during flight are:
   - *Weight* – has a fixed value, being directly proportional with the mass of the blade. Due to the positioning of the anti-torque rotor in a vertical plane, the force of gravity acts in this plane, having a different orientation in relation to the position of the anti-torque rotor blade, which is in rotational motion.
   - *Lift* – represents the aerodynamic force generated by the flow of a fluid around a surface, being, as an orientation, perpendicular to the direction of the flow of the fluid. The lift generated by an airfoil is influenced by: the speed of the air current, the density of the air, the characteristics of the airfoil and the angle of attack formed by the airfoil chord with the direction of flow of the air current.
   - *Drag* – represents the force that opposes the movement of the blade through the air and is, in direction, opposite to the drag force and the air current. The main types of forward resistance are: profile resistance, induced resistance and parasitic resistance.
   - *Traction* – represents the force generated by the operation of the helicopter's engines. This force is variable in magnitude depending on how the incidence of the blades is varied by the pilot via the ailerons.

B. *Boundary conditions and initial assumptions* – Helicopter flight is a complex phenomenon, in which many external factors are involved, such as: environmental conditions (temperature, humidity, precipitation), the type of flight, the action of unpredictable external forces, as well as gusts environmental wind or impact with foreign objects.

C. *Structural elements* – depending on their characteristics and geometric properties, they give rigidity to the blade to be able to cope with operational demands. The main structural elements are the following:
   - the skin – represents the component that comes into direct contact with the external environment. For this reason, it must be designed to withstand the impact with foreign objects, which can cause damage, and also, to withstand the harshest environmental conditions (extreme temperatures, high humidity, precipitation, etc.). Given the composite helicopter blades, the skin is made by overlapping multiple fabrics impregnated with thermoplastic/heat-resistant resins.
   - the spar – represents the main structural element of strength that spans the entire length of the blade. It is intended to withstand the aerodynamic loads and weight of the blade, which differs depending on its positioning during flight. Within a blade there can be several such structural elements, depending on the intensity of the loads.
   - the inner core – represents the material used to fill the inner cavity of the blade, having structural properties appropriate to the loads that the blade must sustain. The materials most frequently used for this purpose are honeycomb structures or polymer foams.

D. *Minimum mass and maximum performances* – is a basic principle applied for manufacturing aerospace structural elements, which can be achieved through successive optimizations phases, which facilitate similar performances, whilst having a smaller mass.

E. *Manufacturing costs and complexity* – were discussed in the previous sub-chapter, for most materials used in making composite materials.

Metal blades are a technologically outdated solution, given the needs of modern helicopters. They offer poorer performance, a shorter lifespan, and a much higher risk of damage compared to modern composite blades.

In the study carried out by Kovalovs A. [14], aiming to optimize the vibration and noise characteristics of helicopter blades, a blade equipped with a "C" profile spar and a NACA23012 airfoil was used, modeled according to the structural characteristics of the MBB blade. The optimization methodology is based on the finite element analysis, the structure being equipped with piezoelectric actuators, along its entire length.

In Rasuo's article [15], carried out in collaboration with the Aeronautical Department of the Faculty of Mechanical Engineering in Belgrade, a study of the fatigue strength of a composite blade was carried out. The blade consists of the outer skin made by overlapping glass-fiber fabrics oriented at 45° and 0/90° with respect to the longitudinal axis, a resistance spar made of glass rovings, and a phenolic foam or a polyurethane foam for the inner structure, depending on the version of the model made.

In the article by Pflumm T. [16] the composite blade of the UH-60A helicopter was analyzed. The study concentrates on analyzing the influence of material uncertainties and the identification of the structural response and the natural frequencies of the blade. The author proposes a multidisciplinary optimization approach based on three software programs (DYMORE, VABS and SONATACBM), after which he concludes that uncertainties have a considerable effect on the dynamic behavior of the blade and on the stresses produced by vibrations.

In the paper by Miller and Narkiewicz [17] regarding the use of active blade torsional control systems to reduce vibration and noise, the authors show how piezoelectric actuators and piezo-composites can be incorporated to create rotor blades with controllable geometry. The article shows how, for a blade with the same NACA0012 airfoil, active fiber-reinforced composite materials are integrated into the blade's laminated skin, which allowed the blade to twist approximately ±0.4° during positioning in the wind tunnel .

1.4 Additive manufacturing in aerospace production

According to the international standard ISO/ASTM 52900 from 2015, additive manufacturing is defined as the process of joining/combining materials to make components based on a 3D model, being manufactured, as a rule, by successive overlapping of material layers [18].

Additive manufacturing is considered one of the industrial revolutions still in progress. Classic manufacturing technologies require the use of large amounts of energy and resources to achieve a high level of manufacturing precision through processes that involve extracting, joining, welding and shaping materials. Recently developed additive manufacturing processes have involve the successive overlapping of layers of material, based on a 3D model designed in specialized software programs.

In choosing the optimal method of additive manufacturing, the following aspects must be taken into account:

- The degree of finishing (physical appearance) of the manufactured parts;
- Materials that can be used;
- Resistance of manufactured parts;
- Print speed;
- Manufacturing temperature;
- Practicality.

In the aerospace domain, the main requirements for 3D printing are high thermal and mechanical resistance and low mass. The use of polymers, as well as different metals, such as titanium or nickel alloy, represents the main current implementation direction regarding aerospace structures 3D printing.

Additive manufacturing offers several competitive advantages over classical manufacturing methods, such as adaptability to complex geometry and customization of the model to be manufactured. Also, depending on the technical requirements, the products are built so that they have a low mass, can be made of several materials, have an ergonomic character, being based on an appropriate combination of different manufacturing processes and the use of the optimal material. Due to the development of these manufacturing processes, additive manufacturing methods are now comparable to classical manufacturing methods, which involve material removal.

Fused Deposition Modelling (FDM) is a process developed by Scott Crump and implemented by Stratasys Ltd. in the 1980s. This method represents the most affordable method for rapid prototyping from a commercial point of view, as well as from a financial perspective. The products are made by extruding the filament, previously heated to its melting temperature, and placing it in successively overlapped layers of material. The main advantages of the additive manufacturing methods used for aerospace structures were presented in more detail in the Scientific Bulletin of the Naval Forces [19].

An important characteristic of parts made by additive manufacturing, which must be taken into account, is their anisotropy, namely, the dependence of physical properties on the orientation of the part at the time of manufacture. The effect can be seen especially in thermoplastic extrusion parts.

1.5 Conclusions

Composite materials are currently used on a very large scale in the aeronautical industry and overcome performance barriers, a factw that would not have been possible using conventional materials. The material created using different constituents is a "hybrid" material, which has improved structural properties.

The most important advantage of composite materials is the significant mass reduction, a key factor for aeronautical structures, representing also a decrease in weight of the aircraft. Also, fiber-reinforced laminated composites are stronger than aluminum, used on most aircraft as the main structural strength material, offering in addition satisfactory aerodynamic characteristics, able to contribute to the reduction of drag and, implicitly, to the reduction of fuel consumption. Composite materials are not affected by corrosion, like metal structures, and have a longer service life (technical resource) than aluminum components, which means lower maintenance costs.

In this chapter, the constructive configurations available for aeronautical blades were analyzed, with the scope of improving their performance characteristics, in order to replace the current manufacturing materials with ones with superior properties.

The current structure of the anti-torque blade provides a balanced character for the operating conditions of the IAR330 helicopter, thus making it viable to maintain the aerodynamic and structural characteristics, while introducing high-performance composite materials in order to increase its performance.

2. THESIS OBJECTIVES AND STRUCTURE

2.1 THESIS OBJECTIVES

The general objective of the doctoral thesis is to develop an alternative constructive solution, made from composite materials, with the aim of replacing the metallic anti-torque blade currently used by the IAR330 helicopters of the Romanian Air Force. The proposed constructive solution will include the advantages of using modern composite materials, together with additive manufacturing technology through 3D printing, to obtain a final product with a considerably reduced mass, but with superior mechanical characteristics.

Main specific objective:

- In-detail study of the existing constructive variants, the variety of materials, as well as the manufacturing methods available for blades composite, in order to choose the best solution which satisfies the strength and mass requirements;
- Experimental validation through the use the wind tunnel, of the aerodynamic pressure distribution on the outer surfaces of the tail rotor blade, determined by using a FEA program to model the fluid flow.
- Determining the mechanical characteristics for each material type used in manufacturing the composite blade and using the obtained results, to validate the numerical analyses carried out with the finite element method;
- Manufacturing the tail rotor blade on a scale of 1:3 and evaluating the its performances from an experimental point of view, by applying an bending force on the free edge;
- Finite element modeling of the anti-torque blade, both in the composite version and in the metallic version, and realizing the comparative analysis of the stresses and deformations obtained for different air flow incidences within the pitch range of the tail rotor blade;

2.2 THESIS STRUCTURE

The doctoral thesis is organized in eight distinct chapters, developed according to the specific objectives and the proposed study directions, in order to achieve the main goal, to demonstrate the viability of a composite configuration of the tail rotor blade of the IAR330 helicopter.

- **CHAPTER 1 – THE CURRENT STATE OF RESEARCH,** represents a synthesis of the main materials used in the construction of propulsive blades intended for the aeronautical industry, from the chronological point of view, but also with respect to the mechanical characteristics. In this chapter, a comparative analysis of the current materials used for the manufacture of blades is presented, with an emphasis on highlighting the main advantages and disadvantages, as well as the defects characteristic of the materials in their composition.
- **CHAPTER 2 – OBJECTIVES AND ORGANIZATION OF THE THESIS**, contains a summary of the main objectives (general and specific) pursued by the doctoral thesis, with a detailed and well-argued presentation of the theoretical and experimental research covered in each chapter.
- **CHAPTER 3 – ASSESING THE PERFORMANCES OF THE METAL TAIL ROTOR BLADE BY FINITE ELEMENT ANALYSIS,** was centered around the study of the mechanical behavior of the tail rotor blade made in accordance with the general dimensions, taken from the manufacturer's execution drawings. The internal components of the blade are characterized by the materials properties used by the manufacturer, in order to provide a set of

reference values of the essential mechanical parameters (mass, stresses, deformations) for future comparison purposes.

- **CHAPTER 4 - EXPERIMENTAL VALIDATION OF AERODYNAMIC LOADS USING THE WIND TUNNEL,** aims to present the experimental instrumentation and the methodology used to determine the pressure field acting on the blade during a constant fluid flow around the blade, at specific incidences and air flow speeds.
- **CHAPTER 5 – DETERMINING THE MECHANICAL AND THE ELASTIC CHARACTERISTICS OF THE MATERIALS USED IN THE COMPOSITE ANTI-TORQUE BLADE,** begins by justifying the choice of materials that will make up the composite blade. The main types of experimental tests used to determine the mechanical characteristics of each material are presented, performed according to the type of applied load (tensile test, compression, bending). The laboratory equipment used for the experimental activity is presented, with special emphasis on the digital image correlation technique (DIC) used to determine stress and strain.

The experimental tests were carried out in accordance with the requirements of international standards for each type of test, namely ASTM C365 for compression testing of sandwich structures, ASTM D790 for three-point bending of fiber-reinforced composite materials and ASTM 3039 for tensile testing of composite materials with polymer matrix. For the thermoplastic polymer used to make the honeycomb core, the orthotropic character of the material was studied depending on the extrusion direction.

- **CHAPTER 6 – FINITE ELEMENT MODELING AND ANALYSIS OF MATERIAL TESTS. VALIDATION OF THE RESULTS BASED ON EXPERIMENTAL DATA,** presents the reproduction by the finite element method of each type of experimental test and the validation process, with respect to the experimentally determined values. It is regarded as a phase before the numerical analyzes of the composite blade, which gives more confidence in its ability to provide reliable results, with a high degree of precision.
- **CHAPTER 7 –COMPOSITE TAIL ROTOR BLADE - MANUFACTURING AND EXPERIMENTAL TRYOUTS. VALIDATION OF THE FINITE ELEMENTS ANALYSIS RESULTS ,** describes the main steps taken to realize the composite blade at a scale of 1:3with respect to real dimensions. The manufacturing technologies for each individual component of the blade are described: the "hand lay-up" method for the skin and for the spar, and FDM thermoplastic extrusion for the honeycomb core. The first performance evaluation stage involved the experimental testing of the composite blade by applying an eccentric force and the validation of the specific numerical analysis based on the experimental data. Due to a satisfactory similarity of the two results sets, the effect of the aerodynamic forces on the composite blade was studied, for different incidences and air flow velocities.
- **CHAPTER 8 – FINAL CONCLUSIONS. PERSONAL CONTRIBUTIONS AND FUTURE PERSPECTIVES**
- **,** has the role of highlighting the main achievements of the scientific research process. The main conclusions obtained during the research stages are presented, which justify and support the constructive variant chosen for the composite blade, as well as the viability of the practical implementation of this model.

3. CHAPTER 3 – ASSESING THE PERFORMANCES OF THE METAL TAIL ROTOR BLADE BY FINITE ELEMENT ANALYSIS

3.1 Main characteristics of the IAR330 helicopter. Operating principles

The IAR330 helicopter has been produced since 1974 by the Romanian Aeronautical Enterprise - S.C. IAR S.A. Brașov, based on the license purchased from the French company Aérospatiale. The factory produced in total over 160 helicopters, of which approximately 57 were destined for export to various countries, such as: Pakistan, Ivory Coast, Sudan, Ecuador, E.A.U. etc.

The anti-torque rotor is the assembly mounted at the tail beam end of the helicopter, which rotates on a horizontal or approximately horizontal axis. Its positioning and distance from the helicopter's center of gravity, allow it to develop a thrust force that compensates for the reactive torque generated by the helicopter's main rotor.

The construction of the anti-torque rotor is simpler than that of the main rotor, because it allows up to two degrees of freedom. It is controlled by the pedals, which doses the power transmitted to the rotor by changing the pitch of the blades, thus controlling the aircraft on its axis of rotation.

The transmission of power to the anti-torque rotor is carried out starting from the main transmission box, by means of transmission shafts, to the rear transmission box, positioned at the end of the anti-torque rotor. The drive shafts are joined by couplings, which give flexibility to the horizontal drive. The role of the rear gearbox is to reduce the power provided by the engines, according to a well-established reduction ratio, in order to provide the optimal rotational speed of the anti-torque rotor.

The blade pitch modification mechanism uses a control system based on cables/control rods, which links the command received from the paddles to the drive mechanism within the anti-torque rotor. The system uses a hydraulically actuated device to reduce the pilot's effort at the helicopter handle.

The main components of the anti-torque rotor are:

1) anti-torque rotor blades - by positioning them on the rear rotor hub, they give the anti-torque rotor a diameter of 3.042 m;
2) rear rotor hub - serves as a support for mounting the blades and allows changing their pitch;
3) rear transmission box - transfers the power received from the engines to the anti-torque rotor and reduces the speed to 1278 rpm, to allow operation in optimal parameters.

Currently, the IAR330 helicopters used by the Romanian Air Force have anti-torque rotor blades made of aluminum alloys. Although there is the possibility of replacing them with composite blades, in previous upgrades of the helicopters the switch was made only for the main rotor blades of the helicopter.

The main structural elements of the anti-torque rotor blades shown in figure 3.1 are: the spar, the skin and honeycomb. The spar is the main structural element of resistance of the blade. It has two holes at its base, which allow the blade to be fitted to the rear rotor hub of the anti-torque rotor. At the opposite end the counterweights of the blade are mounted. The skin is what gives the blade the shape of the aerodynamic profile, being disposed from the leading edge of the blade to the trailing edge, both on the inside and outside of the blade. The rigidity of the blade is achieved by using the NIDA core. The salmon is an element located at the free edge of the blade and plays a role in its aerodynamics.

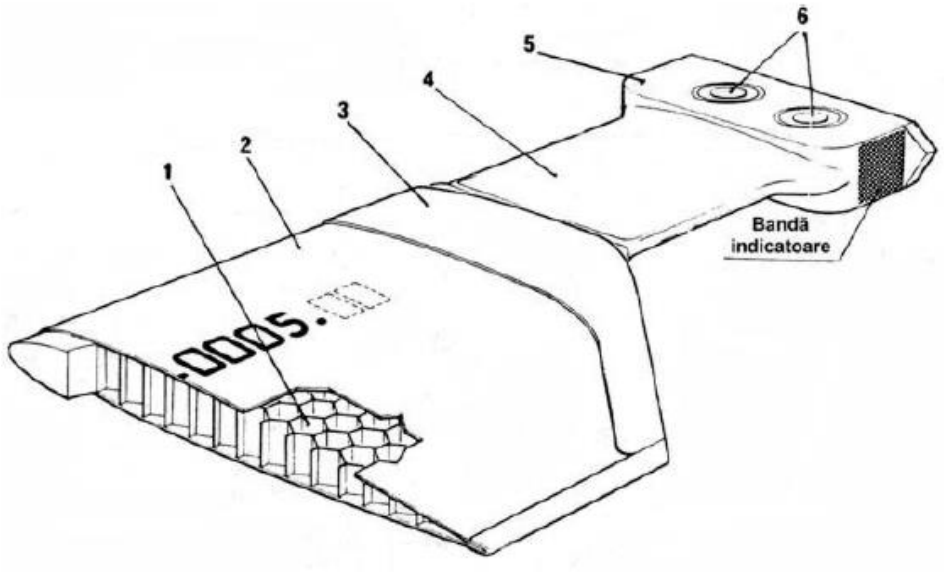

Fig. 3.1 The main structural elements of the anti-torque rotor blade [21]

The IAR330 helicopter currently uses metal blades to equip the anti-torque rotor. The main metal alloys used in the construction of these blades, classified according to the structural components, are:

A. *The skin* - made of aluminum 6061-T4, with a thickness of 0.5 mm. The alloy was developed in 1935, with magnesium and silicon as the main component elements. It has good mechanical properties, is easy to weld and is most often extruded to obtain the necessary components.
B. *The spar* - the main resistance element of the rotor blade. It is made of aluminum alloy 6061-T6511, subjected to heat treatment and artificial aging. The final component made from this alloy is obtained by extrusion.
C. *The honeycomb core* - made of aluminum alloy 5052, extremely resistant to corrosion and used especially in the marine environment. It has a high concentration of magnesium, making it the strongest non-heat-treated aluminum alloy. The material is easy to process for making mechanical components, it is easy to weld and easy to use for making intrinsic structures. Honeycomb structures made from this material provide the aerospace industry and the commercial environment with a high degree of flexibility for making structures that require relatively little mass. The material used to make the honeycomb core of the IAR330 helicopter is NIDA 2.3-3/8-.0015 P(5052).

3.2 Determining the pressures exerted by the air flow on the surfaces of the blade, depending on its incidence, using the Fluent program

The anti-torque rotor of the helicopter has, during the hover flight of the helicopter, a constant speed of approximately 1278 rpm. The value of these pressures can be determined by using the "Fluent - Fluid Flow" module within the Ansys Workbench program.

Due to the fact that the incidence of the blade plays an essential role in the differential distribution of the pressures determined by the air current on the blade surfaces, in the study of the air flow and for the determination of the pressures on the blade surfaces, its variation must be taken into account. The anti-torque rotor of the IAR330 helicopter allows a variation of incidence (α) of approximately 18º, within the range **+2.5º ÷ -15.5º**. The aerodynamic study of the three-dimensional flow, presented in this subsection, was carried out for the following four values of the incidence of the anti-torque blade:

a. **$\alpha = +2,5^o$** - represents the maximum positive incidence that the anti-torque blade can adopt, based on the command received from the pilot's;
b. **$\alpha = 0^o$** - the value at which the pressure distribution is symmetrical on both sides of the anti-torque rotor blade, the maximum load being taken over by the leading edge;
c. **$\alpha = -6,5^o$** - important from a practical point of view, because it represents the incidence at which the helicopter maintains its stable position around its axis of rotation;
d. **$\alpha = -15,5^o$** - represents the maximum negative incidence that the anti-torque blade can adopt, based on the command received from the pilot's handle.

The symmetry of the aerodynamic profile used to create the blade implies that its incidence can be modified without taking into account the sign (positive/negative). The motivation is represented by the fact that the study aims to determine the distribution of the pressures exerted by the air stream, as well as, subsequently, the maximum strains and stresses, thus being irrelevant for this study on which faces of the blade the fluid pressure acts.

Taking into account the fact that the distance from the base of the blade to its axis of rotation is approximately 276.7 mm and knowing the length of the blade of 1266.30 mm, we can obtain the total distance from the tip of the blade to the axis of rotation is 1543 mm. This results in an air flow velocity around the blade of approximately 206.50 m/s, corresponding to the free end of the blade. For the air flow analysis in the numerical simulations, an air speed of 50 m/s will be used, because this speed value represents the maximum that can be validated experimentally, within the wind tunnel, without risking irreversible damage to the anti-torque blade model.

A standard k-ε type turbulent viscosity flow model was used within the Fluent program, in order to determine the pressures created by the airflow on the blade surfaces. This mathematical model is one of the most widely used option for the studyingf turbulent flows. It is a semi-empirical model, which uses transport equations to determine the kinetic energy of turbulence (denoted by "k") and their dissipation rate (denoted by "ε").

Within the flow environment, the fluid is considered to be air, characterised by the standard pressure and temperature parameters measured at sea level:

- Fluid pressure – 101,325 kPa;
- Fluid temperature – 15^{o}C;
- Fluid density – 1,225 Kg/m^3.

To carry out the analysis, the following assumptions were made: there is no heat exchange with the outside environment, and the air flow speed is constant along the entire length of the blade.

The simulation of fluid flow having zero incidence with respect to the blade chord is characterized by a potential (irrotational) flow, where all components of the rotational angular velocity are approximately zero. The maximum static pressure is 15.25 kPa and is located on the leading edge of the anti-torque rotor blade, and the minimum pressure is found on the blade foot. The maximum negative static pressure is found in a limited area at the bottom of the blade foot and is due to the geometrical modeling, which is why it will not be taken into account in the static analysis.

The flow of air around the blade positioned at a zero degree angle of attack is illustrated in figure 3.2, where the boundary layer and its disposal around the airfoil of the blade can be seen.

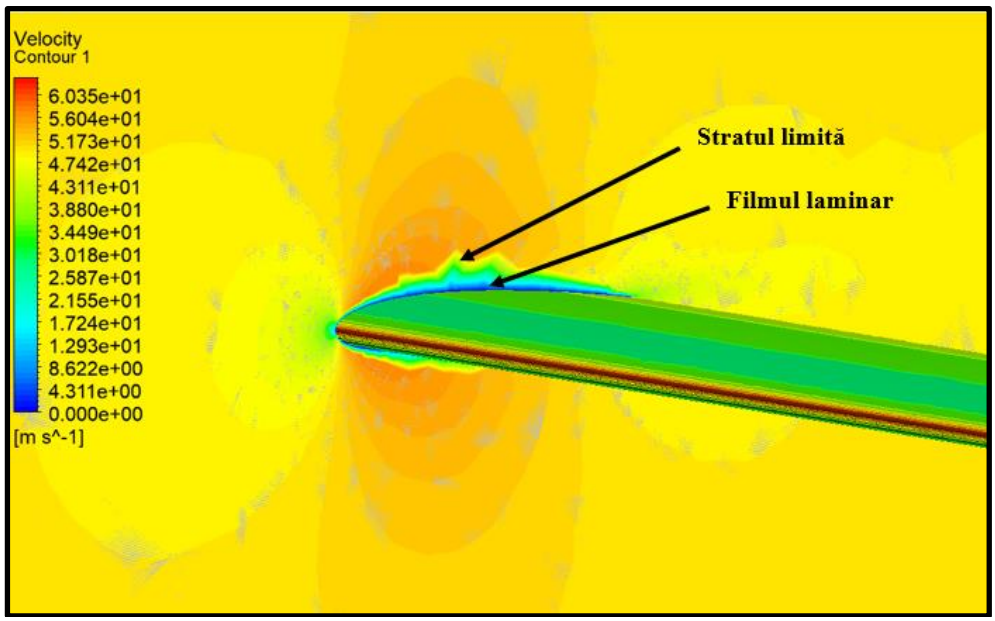

Fig. 3.2 The velocity variation of the fluid traversing the skin of the tail rotor blade at $\alpha = 0^{o}$

The boundary layer represents the region where the fluid velocity changes due to the interaction with the airfoil, being located between the surface of the blade cover and the area where the velocity gradient becomes zero. It represents the area where the effect of the walls is manifested, resulting in the dissipation of the mechanical energy of the fluid.

The laminar film is the area immediately adjacent to the shell where the flow remains laminar. For the case of zero incidence, it extends from the leading edge to the trailing edge, having an approximately constant size. The separation of the boundary layer occurs at the intersection of the fluid with the leading edge, causing the appearance of the turbulence zone located on both sides of the blade, at a certain distance from the laminar film.

The appearance of turbulence can be observed on both sides of the blade skin, as a results of the fluid flow impact with the blade skin. Given the symmetrical aerodynamic profile, the displacement of the fluid is carried out identically on both sides of the anti-torque blade. The contour lines of the pressure distribution have an approximately linear shape, contributing to a clear delineation of the main pressure areas, according to the color codes. The dominant values, according to the obtained results, are those in the middle zone of the pressure range.

Basically, the separation of the boundary layer occurs when the pressure of the fluid outside it increases in the direction of travel, the velocity of the fluid suddenly changes. In this case, the detachment occurs at the intersection of the fluid with the leading edge, causing the appearance of the turbulence zone located in the vicinity of the leading edge. The turbulent flow does not amplify to the shell due to the low velocity, which cannot sustain the turbulence.

The presence of turbulent flow can be observed, which is characterized by a movement along irregular trajectories of the fluid, with different speeds. The transition from the laminar flow to the turbulent flow occurs gradually, noting the presence of a zone of transient displacement of the fluid.

By means of a parametric analysis, the variation of the aerodynamic pressure in relation to the incidence of the air current was determined, for the speed of 50 m/s used in order to validate the aerodynamic pressures, as well as for the speed of 206.5 m/s corresponding to the maximum tangential speed at the tip of the blade.

The evolution of the main aerodynamic forces acting on the anti-torque blade, represented by the lift and the drag, was represented graphically in relation to the variation of the angle of incidence made by the anti-torque blade with the direction of air flow.

The graphic evolution indicates a decrease in the average value of the static pressure, along with the increase in incidence α, due to the intensification of areas with negative pressure, as an effect of the separation of the laminar layer and the appearance of turbulence. It is also observed that the maximum pressure is manifested for the symmetrical orientation of the blade in the air stream (α=0°), in the area of the leading edge of the anti-torque blade.

The value of the lift force corresponding to the maximum incidence is approximately ten times higher than in the case of zero incidence. The destructive effects of the air current are felt for high values of incidences and aerodynamic forces. The results obtained using the Fluent program will be entered into the static analyses, to evaluate the response of the metal blade with respect to the aerodynamic stress.

3.3 Static structural analysis of the tail rotor blade

The tail rotor blade is one of the helicopter components subjected to continuous stress during the helicopter's flight, the degree of stress being influenced by numerous factors, among the most notable being:

- environmental factors (temperature, atmospheric pressure, humidity);
- impact/interference with various foreign bodies;
- modification of the aerodynamic characteristics along the length of the blade (pressure distribution, air flow around the blade), caused by wind gusts or the modification of the incidence of the blade;
- modification of the incidence of the blade, commanded controlled by the helicopter pilot.

In this subchapter, the finite element analysis of the anti-torque blade is based on the geometric model of the blade positioned in the vertical plane, with the air stream having a uniaxial direction of flow, from the leading edge to the trailing edge. This arrangement was chosen for practical reasons, given the limited possibilities of validating the aerodynamic loads in the case of rotation of the anti-torque blade at the nominal operating speed. Thus, the static analysis was carried out for the same layout of the blade inside the wind tunnel, which will be presented in the next chapter, for the experimental validation of the pressures exerted by the air current on the blade envelope. The static analysis was carried out for the four reference values of the incidence range of the anti-torque blade of the IAR330 helicopter, respectively 0º, 2.5º, 6.5º, 15.5º.

The mechanical properties provided by the manufacturer for each type of aluminum alloy are assigned to each structural component in the finite element numerical analysis, as follows:

- the spar – aluminum alloy 6061-T6511;
- the honeycomb core – aluminum alloy NIDA 2.3-3/8-.0015 P(5052);
- the skin – aluminum alloy 6061-T4.

In the case of helicopter hover flight, the forward speed of the helicopter is considered null, the helicopter being practically suspended in the air, at a constant distance from the ground. The rotor blade is loaded by the aerodynamic pressure generated by the air current, under the conditions of a constant velocity flow of approximately 50 m/s. This speed was chosen for practical reasons, due to the limitations imposed by the vibration of the tail rotor blade, known in aerodynamic terms as "flutter". This represents a state of instability for the aerodynamic structure, a state that determines the sustained oscillation of the structure, by taking the necessary energy from the air current.

The aerodynamic pressure distribution along the blade was determined for an air flow incidence $\alpha = 0^{\circ}$, the areas being delimited by the constant pressure lines. Maximum static pressure is located in the frontal area of the anti-torque blade, in relation to the direction of the air current, especially in the area of the leading edge.

The maximum equivalent stresses are present on the body of the honeycomb structure, at the wall intersection areas of the hexagonal cells, reaching the maximum value of 9.11 MPa, for the flow case described previously. The resistance spar, as the main stiffening element, takes the aerodynamic load, being subjected to a bending moment that compresses the lower blade spar on the opposite of the air flow direction. The stresses are also distributed on the leading edge of the spar, similar to the outer skin, being the main area of contact of the air flow with the anti-torque blade.

The tendency of the maximum stress to increase with the increase in incidence was comparatively presented for each of the four studied values of the incidence, in relation to two air flow velocities:

- linear air flow, at a constant speed v=50 m/s;
- the linear flow of the air current, with a constant speed v=206.5 m/s, corresponding to a linear speed obtained at the tip of the blade, in the case of the operation of the anti-torque rotor at a speed of 1278 rpm.

According to the results obtained, the linear air flow at the tangential speed of 206.5 m/s leads to the appearance of stresses well above the resistance limit of the aluminum alloys used for the blade, therefore not being viable to reproduce from a practical point of view, by studying the air flow with the help of the wind tunnel. The linear flow is carried out strictly with a comparative role, in order to evaluate the performance of the final composite blade.

Among the three structural components, the resistance spar and the honeycomb take the largest share of the specific deformations, with the blade sheath being located at the opposite pole. The maximum deformation was identified on the honeycomb core, in the area of the trailing edge, more exactely, in the vicinity of relatively small surfaces.

The numerical analysis carried out on the anti-torque rotor blade made of aluminum alloy highlights the fact that increasing the incidence of the blade has the effect of a directly proportional increase in the values of stresses and related deformations. The maximum displacement obtained in the case of linear flow is located at the free extremity of the anti-torque blade, which is deformed according to the direction of movement of the air current.

In all calculation cases, it was possible to observe the distribution of significant stresses on the foot of the blade, in the area with the smallest cross-section, which is why the manufacturer used the most resistant material in the entire structure (aluminum alloy 6061-T6511) to counter the moment bending created by aerodynamic loading. Regardless of the helicopter's flight regime, the spar represents the most resistant structure, which takes the largest portion of the stresses. The influence of different inner filler materials was also studied to evaluate their influence on the overall performance of the blade [22].

Considering the results of the numerical analyses, regarding the effect of the aerodynamic loading of the blade at different incidences and air flow speeds, it can be stated that the maximum speed, from the safety point of view, for which the practical validation of the aerodynamic loading will be carried out is of 50 m/s, for a maximum incidence α=6.5º. Up to these thresholds, the materials that make up the anti-torque blade model are within the allowable strength limit provided by the manufacturer.

3.4 Conclusions

The IAR330 helicopter employed by the Romanian Air Force's is a transport helicopter, manufactured in multiple equipment variants, depending on its mission. It has been serving the Romanian Air Force for over four decades, during which it has demonstrated its practical capabilities, going through several modernization stages. The helicopter's main rotor uses blades made of composite materials, while the tail rotor blades are made of metal alloys. The SA 332 helicopter is the French improved version of the IAR330 helicopter, which uses composite tail rotor blades.

By using finite element analysis software programs it was possible to create a full-scale geometric model of the IAR330 helicopter blade that respects the overall dimensions and structural characteristics. The modeling involved designing the main resistance elements of the blade (spar, honeycomb core and skin), and then uniting them into a single assembly.

The numerical analyses carried out indicate the intensification of the maximum deformations and the maximum equivalent stresses, with the increase of the incidence of the blade. Considering the results of the numerical analyses, it is necessary to limit the experimental air flow speed to the value of 50 m/s, and the incidence of the blade at $\alpha=6.5^{o}$, so that the experimental tests can be carried out in safe conditions, without the tail rotor blade pattern being completely damaged. The mechanical characteristics of the materials used allow such tests to be carried out, according to the results obtained in the static analyses.

The advantages of using composite materials, such as the reduction of mass brought to the helicopter structure, corrosion resistance and superior strength characteristics compared to the traditional metals used, make them the desirable solution for any modern aircraft. In the case of aircraft made of metal components, the vast majority of operators opt, as far as the resistance structure allows, for the transition to components made of composite materials. The mechanical characteristics offered by these materials are clearly superior to any other material previously used for aviation structures, and the possibility of their use together with systems for monitoring the state of structural integrity, give them the opportunity to become "smart" materials, in the true sense of the word.

4. EXPERIMENTAL VALIDATION OF THE AERODYNAMICS LOADS BY USING A SUBSONIC WIND TUNNEL

4.1 Main forces which act on the tail rotor blade according to the flight conditions

The main aerodynamic forces acting on the helicopter are: traction, drag and lift (fig. 4.1). Understanding how these forces act and how they can be controlled, coupled with the proper use of flight controls, is essential to the safety of helicopter flight.

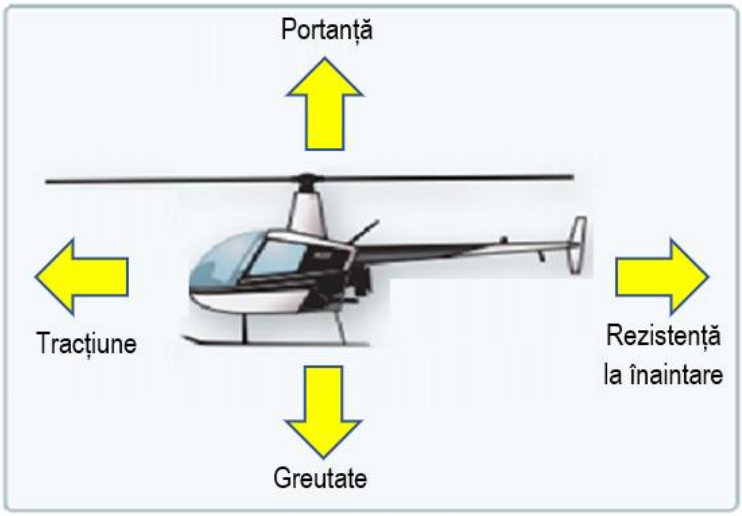

Fig. 4.1 The main forces acting on the helicopter

Thrust is the force produced by the helicopter's engines. It is, in sense, opposite to the forward resistance and in magnitude, greater than it. In principle, it acts parallel to the longitudinal axis of the helicopter.

Weight is the force acting on the aircraft from the center of gravity, in a vertical, downward direction, being opposite to lift, as an orientation. Its value is considered to be fixed, determined according to the mass of the helicopter, fuel and passengers. In order to move, the helicopter must generate enough lift so that it can overcome the total weight of the helicopter.

Lift is the force produced by the dynamic effect of the air on the airfoil, which acts from the airfoil center and is oriented perpendicular to the helicopter's flight direction. It is generated when a body changes the direction of fluid flow. When the body and the fluid are in relative motion relative to each other, and the body causes the direction of the working fluid to become perpendicular to the initial direction, a force opposite in direction, called lift, appears.

A symmetrical airfoil must have a positive angle of attack so that lift is generated. For a zero angle of attack, no lift is generated, and for a negative angle of attack, the lift is also negative. For cambered or non-symmetrical airfoils, lift can be produced even at zero or slightly negative incidence.

Drag is the force oriented against the direction of the air current, which opposes the movement of the helicopter through the air and is caused by the non-uniformity of the flow around the wing, rotor, fuselage, etc. [2. 3].

The drag coefficient is a dimensionless coefficient, which depends on the geometry of the studied body, in its determination taking into account both the skin friction and the profile resistance. It generally depends on the Reynolds number.

The total forward resistance is the sum of the three resistance components (induced resistance, parasitic resistance, and form resistance). As the speed increases, the parasitic

resistance increases, while the induced resistance decreases. The drag, however, remains relatively constant throughout the speed range, with a slight increase at high speeds.

4.2 Main helicopter flight conditions

Hover flight is the most difficult type of flight to be performed by a helicopter, from a pilot's perspective. This is because the helicopter generates its own airflow, which acts vertically downwards against the fuselage of the helicopter. In order to keep the helicopter in a fixed position, it is necessary for the pilot or the automatic flight control systems to make continuous corrections and changes. As a rule, hover flight is performed at a relatively small distance from the ground.

The helicopter tail rotor aims to produce a thrust force opposite in orientation to the torque generated by the main rotor [24, 25]. This force is sufficient to move the helicopter sideways. According to Newton's third law, which states that for every action there is an equal and opposite reaction, the rotary motion of the main rotor in a certain direction causes the fuselage of the helicopter to rotate in the same direction. The amount of torque depends largely on the power available to the engines at the time. In order to control this phenomenon, it was necessary to develop the anti-torque rotor, the traction generated by it can be controlled by the pilot by means of the paddles.

The translational tendency is the phenomenon whereby, during flight of a helicopter with a single main rotor, it tends to move in the direction of the thrust of the anti-torque rotor. To prevent this phenomenon, there are several constructive solutions that can be adopted, such as mounting the horizontal transmission at a certain angle, so that the anti-torque rotor has a certain degree of inclination.

The vertical flight of the helicopter is achieved starting from the flight to the fixed point. By increasing the incidence of the rotor blades while keeping the rpm constant, the helicopter gains a climb rate, and if the incidence of the blades decreases, the helicopter will descend.

Forward flight is that flight in which there are no changes in air speed and the four aerodynamic forces are in balance. In unaccelerated forward flight, on a constant trajectory and constant speed, lift equals weight mode and thrust equals drag mode.

The airflow over the helicopter rotor differs depending on the helicopter's flight regime. In forward flight, the airflow flows in the opposite direction to the helicopter's direction of travel, with the air speed equal to the helicopter's travel speed. Due to the fact that the rotor is in a circular motion, the speed of the airflow over a blade depends on: the position of the blade in the plane of rotation at a given moment in time, the rotational speed and the speed of the helicopter.

Lateral flight involves tilting the plane of the main rotor in the direction in which the helicopter is desired to travel. In this flight, the directions of lift and weight forces remain unchanged, but thrust acts in the direction in which travel is desired, with drag acting in its opposite direction. This type of flight can be unstable, due to the parasitic drag of the fuselage, combined with the lack of horizontal stabilizers normally used to facilitate movement in the direction of flight. Increasing altitude makes it easier to do this type of flight.

Backward flight involves tilting the main rotor plane backward in the backward direction, the vectorial resultant of thrust and lift forces being thus oriented in the same direction. This flight requires increased attention as the tail beam of the helicopter tends to tilt downward. A prior research of the area in which this type of flight is to be carried out must be carried out, flight at a higher altitude being the indicated solution in such situations.

4.3 Types of fluid flow used to determine the pressure distribuition. Two-dimensional study of the fluid flow

When analysing fluid flow in a certain area there are many variables that must be considered in order to perform an effective aerodynamic study. The variation of certain parameters, such as the density or velocity of the fluid, leads to the classification of different types of flow, necessary for a better understanding of how the fluid interacts with different aerodynamic bodies.

Incompressible flow is that type of flow of a fluid that maintains its constant density. From a practical point of view, incompressible flow is not possible, but in the study of aerodynamics, when the air speed is less than Mach 0.3 (about 370 km/h), the fluid flow process is assumed to be isochoric (volume constant). The incompressibility of the fluid assumes that its density remains constant over a certain portion of the fluid, which moves with the speed of the entire flow.

Compressible flow is characterized by changes in fluid density relative to the distance traveled by the fluid. A concrete case would be that of the fluid flowing over a body, with an increase in fluid density at the point of impact of the fluid with the body [26]. Flows with a Mach numbers less than 0.3 are considered incompressible flows because the change in density due to velocity is about 5%.

In numerical simulations, turbulent flow at low Reynolds numbers can be described using the Navier-Stokes equations. The main restrictions in performing such a simulation are the computing power of the processing unit and the efficiency of the algorithm used to determine the solution. In many cases, experimental results have been shown to coincide with numerical analysis results. It is the value of the Reynolds number that determines whether a flow is laminar or turbulent.

The displacement of any fluid is a fluid dynamics problem, which can be described using the Navier-Stokes equations [27]. This equation is the result of applying Newton's second law to the fluid.

Laminar aerodynamic profiles, such as that of the anti-torque rotor blade, are characterized by a predominantly laminar layer on the upper skin of the blade. These profiles still show separation of the air current and turbulence, but at higher values of the angle of incidence α. For low values, the airflow accelerates and the negative pressure gradient on the extrados causes separation to be avoided.

Fluid flow in a two-dimensional (transversal) plane facilitates profile visualization of the displacement of the fluid in the flow domain, relative to the angle of incidence of the blade. Thus, we can determine certain characteristics of the flow, such as: the conditions that facilitate the emergence of turbulence, the detachment of the boundary layer from the body of the aerodynamic solid, the location and evaluation of the intensity of the turbulent flow, etc. The default conditions to characterize the flow type are as follows:

- ambient temperature: 15°C;
- air density: 1.225 kg/m3;
- Reynolds number: $3 \cdot 10^6$;
- the angle of incidence of the air stream against the anti-torque blade: $0^o \div 15.5^o$;
- flow model: k-ε;
- Mach number: 0.15 (corresponding to a speed of 50 m/s).

The previously specified Reynolds number was chosen taking into account the flow velocity and airfoil chord size. This measure characterizes the viscosity as well as the compressibility of the fluid through which the aerodynamic solid moves, which in this case is air. Its value is characteristic of a turbulent flow, variable depending on the viscosity of the air. It should be mentioned that the viscosity of the fluid disappears for flows with Reynolds numbers higher than $10 \cdot 10^6$.

Static pressure is represented by the force acting on the airfoil, relative to the unit area. Basically, this parameter represents the pressure exerted by the fluid on the surface of the NACA0012 airfoil, when the air is not moving. If the value of the dynamic pressure is determined, as a parameter dependent on the air density and speed, the total pressure of the air flow, which is variable within the rotational flow, can also be determined.

The variation of the static pressure is illustrated graphically for incidences in the range $0^0 \div 15^0$. Thus, it can be seen how, starting from zero incidence, where the pressure distribution is identical on both sides of the blade, a maximum positive pressure is reached on the lower part of the leading edge, which gives rise to a negative pressure zone on extrados. The area affected by the negative pressure decreases in size as the angle of attack increases, favoring the emergence of turbulent flow, after the value of 12.5^0.

Dynamic pressure is a measure that depends exclusively on the density of the air, as well as its speed. Compared to the previously determined results, it can be seen that it acts opposite to the intensity of the static pressure. Thus, the areas where the static pressure is maximum, located in the direction of the air current, are characterized by a reduced dynamic pressure, given the reduction of the speed of the fluid at the time of its intersection with the aerodynamic profile. It can be seen that the area with reduced dynamic pressure propagates on the face opposite to the direction from which the air current acts, being the upper skin of the aerodynamic profile, in this case. The pressure felt on the upper skin of the profile increases, and the speed of the fluid decreases, which translates into an increase in dynamic pressure.

The results confirm some of the previous conclusions regarding static pressure and dynamic fluid pressure. Increasing the speed in the leading edge area has the effect of increasing the static pressure, and reducing the speed on the face opposite the direction of the air current has the effect of reducing the dynamic pressure. A slight detachment of the boundary layer can be observed, starting with the value of 10^0 of the angle of attack, the flow becoming turbulent when reaching the value of 15^0. This threshold represents the incidence variation limit used mainly in emergency cases, to perform a quick control maneuver around the helicopter's yaw axis.

4.4 Experimental validation of the aerodynamic pressures obtained in Fluent

Wind tunnels are highly advanced scientific equipment used to reproduce the flight conditions of an aircraft or a certain aerodynamic component. In order to carry out these experimental tests, models can be used on a certain scale and if the dimensions of the wind tunnel allow, real models can be used.

The development of these equipment occured in parallel with the aircraft development, being used today not only for aeronautical research, but also for automobiles, high-speed trains, and sports equipment [28].

Depending on the way the air moves, wind tunnels can be classified as closed circuit or open circuit. A model of the tail rotor blade was introduced into the closed circuit wind tunnel located to INCAS (National Institute of Aerospace Research) Bucharest.

The principle of operation of a wind tunnel, in most cases, consists in moving a large volume of air through the inside of a tube in which the model under study is embedded. Studying the movement of fluid around different bodies can be facilitated by the use of smoke or a dye, which allows visualization of the air current. The measurement of the speed with which the air moves in the wind tunnel is realized by using Bernoulli's principle, and the direction of the air current can be determined by devices attached to the aerodynamic surfaces of the body. Liquid bubbles can also be introduced upstream of the air current, in order to follow their trajectory around the studied body.

The pressure distribution on the surfaces of the tested model was determined from the beginning of this type of experiment, by realizing numerous holes in the areas of interest on the

studied body, where tubes are positioned as pressure gauges, which allow the pressure to be measured in each hole. An alternative would be to use a fluorescent paint, which changes its light intensity depending on the pressure level.

The aerodynamic properties of a scaled-down object differ. However, by determining patterns of similarity, a satisfactory correspondence between the full-scale model and the reduced-scale model can be obtained. The most used similarity parameters are:

- geometric similarity, in which all dimensions must be made to the established scale;
- the Mach number, which should be the same for both models;
- the Reynolds number, by observing the ratio between inertial and viscous forces, for both models.

The experimental analysis was carried out in the subsonic wind tunnel, which allows continuous operation at atmospheric pressure, the maximum speed of the air current generated by the wind tunnel being 110 m/s (Mach = 0.32). The test section is solid-walled and has a useful size of approximately 2.5 m x 2.0 m x 4 m. The working circuit of the tunnel is of the closed type and allows reaching Reynolds numbers up to 1.5 million [84]. The main advantage of this type of tunnel is that it requires less energy consumption compared to the open type, but it does not allow the use of smoke to visualize the currents in the test section.

The main flow parameters inside the wind tunnel are as follows:

- Kinematic viscosity – $14{,}7 \cdot 10^{-6}$ m^2/s, at an ambient temperature of 16°C;
- Blade chord – 186,5 mm, for the 1:1 scale blade;
- Ambient air pressure - 101300 Pa, measured at the laboratory;
- Speed of sound - 340 m/s;
- Air density – 1,225 kg/m^3;
- Air flow speed - 30 m/s, 40 m/s, 50 m/s;
- Mach Number – 0,08824, 0,11764 or 0,14705, depending on the fluid flow rate;
- Reynolds Number - 380612, 507483, or 634354, for the three flow rates used.

Holes were created in the skin of the blade model to allow the insertion of static pressure measurement tubes. This arrangement was chosen in order not to influence the characteristics of the aerodynamic flow around the blade, so that the data provided is as close as possible to reality.

The pressure tubes were positioned so as to take the value of the pressure exerted by the air stream, after which to transmit this value to the processing and display unit of the wind tunnel. Ten pressure tubes were used, corresponding to each measurement point on the blade skin, all routed to transmit pressure to the blade foot, to influence the displacement of air currents as little as possible.

Before inserting the blade into the wind tunnel, the pressure tubes were covered with a special foil in order to reduce, as much as possible, the drag caused by this growth.

Due to the symmetry of the NACA0012 airfoil of the blade and to simplify the blade machining process, all air pressure intakes were positioned on one side of the blade skin. In order to obtain the total pressure distribution on all the surfaces of the blade, the incidence of the blade was modified, so that the surface on which the holes are present behaves in turn, both as outer surface and as inner surface.

The blade in its final form was placed inside the wind tunnel and recessed to ensure its stability during testing. This was positioned at an angle of 90º to the horizontal direction, with the leading edge facing the direction of the air current. The mounting device is connected to an actuation mechanism, which allows the variation of the incidence of the blade in relation to the direction of flow of the air flow.

The positioning of the aerodynamic pressure measurement holes was carried out in three cross-sections, in essential points within the attack board, the trailing board, as well as in the

middle area, belonging to the upper/inner skin. Their exact arrangement, in relation to the dimensions of the blade, is shown in figure 4.2.

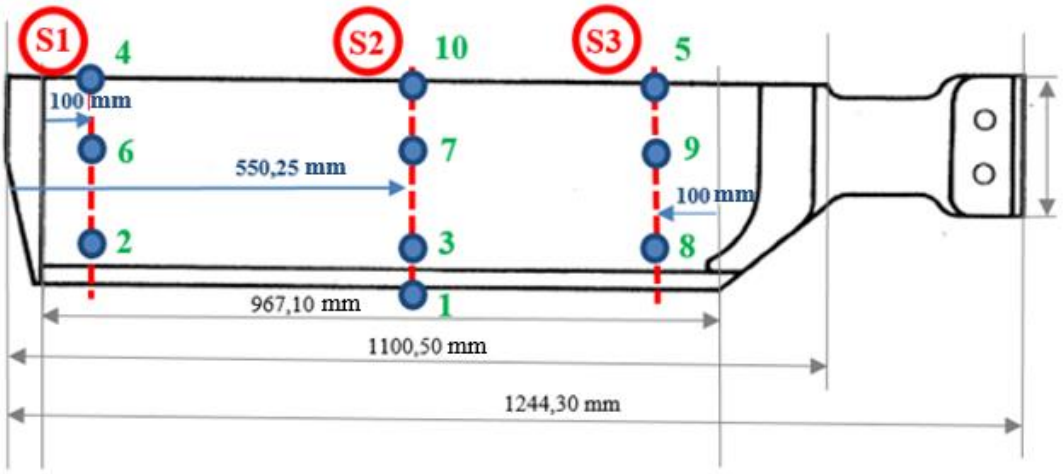

Fig. 4.2 The arrangement of the holes made for measuring the aerodynamic pressure

The incidence of the blade in relation to the direction of movement of the air current represents an extremely important parameter, the change of which depends on the variation of the pressure distribution on the blade surfaces.

In carrying out the experimental analysis in order to validate the results obtained with the Fluid Flow program, three reference values were used within the variation interval of the incidence of the blade +2.5º ÷ -15.5º. These are the following:

- 0º - specific to a symmetrical distribution of pressures on the two faces of the blade;
- 2.5º - the maximum positive value of the blade;
- 6.5º - the value at which the helicopter maintains its stable position in relation to the axis of rotation.

Considering the fact that the incidence value of 15.5º occurs extremely rare in helicopter operation, both in numerical and experimental analysis, this value was not taken into account. Also, the high value of the incidence implies subjecting the anti-torque blade to much higher stresses, and to avoid damage or breaking of the material, it was preferred to carry out the experimental validation for incidence values of maximum 6.5º.

The variation of blade incidence was achieved in relation to the blade's center of pressure, which, for symmetrical airfoils, is located at 25% of the airfoil, relative to the trailing edge, i.e. at a distance of 46.625 mm.

The second parameter in relation to which the experimental analysis was carried out is the speed of the air current. Although, the actual speed at the tip of the blade, during the hover flight of the helicopter, can reach a maximum value of 206.5 m/s, the experimental analysis was performed only for low air current speeds (30 m/s , 40 m/s, 50 m/s), in order to protect the structural integrity of the blade model, subjected to aerodynamic stresses.

4.5 Finite element analysis and experimental results comparison

Comparing the experimentally determined values with the results of numerical analyzes of fluid flow around the blade is an essential step for validating the results of the numerical analysis, so that there is certainty that the studied structure is loaded similar to real cases. Although, in the case of zero incidence, the pressure distribution is symmetrical on both sides of the blade, the maximum value being reached in the leading edge area, increasing the incidence leads to the increase of the area affected by the direct impact of the air current and, simultaneously, to the appearance of a pressure positive, with a negative aerodynamic pressure being generated on the opposite surface.

To facilitate the comparison between experimentally determined results and numerically determined results, the following specifications are required:

- pressure ports numbered 4, 5 and 10 are used to determine the pressure on the leading edge of the blade;
- pressure port number 1 is used to determine the pressure value on the trailing edge of the blade;
- pressure ports with numbers 2, 3, 6, 7, 8, 9 are used to determine the working pressure on the inner side/outer side of the skin of the blade, depending on the incidence of the blade.

With these considerations in mind, the comparison can be made between the two sets of results, for the main areas of interest of the blade: the leading edge of the anti-torque blade, the trailing edge of the anti-torque blade and the trailing edge/inner side of the tail rotor blade.

The results obtained in both cases (numerical and experimental analysis) indicate a trend of pressure increase, proportional to the increase in air speed, the maximum values being reached for an air flow speed equal to 50 m/s.

The maximum positive pressure is located along the entire length of the leading edge of the blade, while the pressures on the leading edge, the leading edge and the trailing edge have predominantly negative values, a fact confirmed by the experimental analysis.

Regarding the incidence of the blade, the general tendency is to increase the pressure on the blade with increasing incidence, for positive incidences, respectively to decrease the aerodynamic pressure, with decreasing incidence, for negative incidences.

Regarding the determined relative errors, it can be stated that the differences found between the values determined experimentally and the results found using the numerical analysis are due to the dimensional approximations of the blade modeled using the finite element method, the determined aerodynamic pressures being nevertheless realistic in value and can be used for the numerical analyzes later of an anti-torque blade, made of composite materials. The results obtained for the area of the leading edge of the blade are the closest in value to the data obtained experimentally, while on the extrados, intrados and trailing edge of the blade appear, in certain situations, relatively large differences, due to the appearance and intensification of turbulence in downstream of the blade and also due to the irregular surfaces located on the blade model used in the experimental analysis.

Considering the fact that the average error for each pressure measurement point is, globally, below 20%, it can be concluded that the two studied cases are comparable in magnitude and that the experimental results validate the results obtained using the numerical analysis.

4.6 Conclusions

In order to carry out the aerodynamic study of a tail rotor blade, it is necessary to understand how the fluid mouves around it and how the fluid interacts with the studied blade.

Numerical analysis through the Fluid Flow module of Ansys Workbench is a good way of determining the pressure distribution on the tail rotor blade surfaces. These values can be used later to study the mechanical behavior of the blade under conditions similar to those during flight.

The use of the wind tunnel belonging to INCAS led to a good experimental validation of the results of the numerical analyses. To enable the comparison between the numerical analysis and the experimental analysis and, at the same time, to perform the validation of the results of the numerical analysis, the two analyzes were carried out for a constant speed along the blade, due to the fact that, by using the wind tunnel within experimental study, the speed variation along the blade is not allowed, similar to the rotating operation of the rear rotor, at a speed of 1278 rpm.

To preserve the structural integrity of the blade, the experimental analysis was performed only for the following air flow speeds: 30 m/s, 40 m/s and 50 m/s.

The aerodynamic pressures obtained from the numerical analysis are similar in value to those obtained from the experimental tests, the reasons for the main differences found between the two sets of results being the small dimensional approximations made in the modeling of the blade, the appearance and intensity of turbulence, the possible slight modification of the aerodynamics of the blade as following the processing of the shell in order to carry out experimental tests, etc.

In conclusion, the two sets of results are similar, thus making possible a further analysis of the mechanical behavior of the anti-torque blade, using the aerodynamic loading determined by means of the numerical analysis.

5. DETERMINING THE MECHANICAL AND ELASTICAL CHARACTERISTICS OF THE MATERIALS USED TO PRODUCE THE COMPOSITE TAIL ROTOR BLADE

5.1 Establishing the manufacturing materials and their position in the composite blade

The research of composite materials with applicability in aeronautical structures, carried out in chapter 1, led to the choice of the following materials, for each component of the anti-torque blade:

- laminated composite material reinforced with carbon fibers for the skin of the tail rotor blade, based on the following components:
  - a Momentum 470-300 epoxy resin matrix produced by Derakane, indicated especially for fiber-reinforced composite materials manufactured by hand using the "hand lay-up" method; according to the technical sheet provided by the manufacturer, it has very good mechanical properties at high temperatures, excellent chemical resistance and better malleability compared to other similar products.
  - a 0°/90° carbon fiber 2/2 twill fabric, model GG285T, manufactured by the manufacturer Castro Composites, having 3000 carbon fibers per filament and a linear fabric density of 200 tex.
- unidirectional carbon fibers (roving) for the spar of the anti-torque blade, the T300 model from Torayca being chosen; the material has been used in aerospace applications for the past 30 years, making it suitable for high-stress applications.
- chlorinated polyethylene filament, containing carbon microfibres, for the creation by thermoplastic extrusion of the honeycomb core of the anti-torque blade; the CPE CF112 Carbon model produced by Fillamentum Manufacturing offered the best value for money to achieve this goal, being indicated for long-term loading applications due to its high wear resistance [29].

Due to the complexity of the orthotropic behavior of composite materials compared to isotropic materials, there are numerous ways in which they can fail, the most important of which are:

- Breaking of the composite material during stretching - it can be due to the breaking of the fibers, due to high stresses in the direction of their arrangement or due to the breaking of the matrix, as a result of stress concentration around the fibers or as a result of high transverse stresses in the direction of the fibers;
- Compressive fracture of the composite material:
  - Compression in the direction of the fibers can lead to their breaking or veiling, as well as to the failure of the matrix due to shearing forces;
  - Compression in the plane transverse to the direction of the fibers can lead to the crushing of the matrix and/or the fibers or the appearance of delaminations;
- Rupture of the material by shear - occurs due to stress concentrators located at the level of the fibers or the matrix.

The technical description of each material was carried out in the following subsections, preceding their experimental testing, to determine the main mechanical and elastic characteristics.

5.2 Determining the mechanical and elastical characteristics of the honeycomb core manufactured by FDM, subjected to tensile and compression loads

The honeycomb structure made by thermoplastic extrusion is used to make the inner core of the blade, located between the strength spar and the thin-walled skin.

The base material chosen for this structure, based on the research carried out in the previous chapters, is a chlorinated polyethylene elastomer (CPE) reinforced with milled carbon fibers, of approximately 100 μm in length. This material is suitable for applications with continuous long-term loads, being characterized by excellent wear resistance, high hardness and satisfactory resistance to most chemical agents.

In order to determine the mechanical characteristics during tensile testing, the INSTRON 8872 static and dynamic axial testing system, equipped with a digital extensometer, was used. One type of specimen manufactured on each direction of material extrusion was studied with the digital image correlation system, to assess how material properties vary with direction of manufacture, as well as to determine Poisson's ratio.

Thus, in order to take into account the orthotropic character of this material, given the random distribution of the carbon microfibers inside it and the way in which their presence and orientation affect the behavior of the material, the thermoplastic extrusion of the samples was carried out in three main directions (fig 5.1).

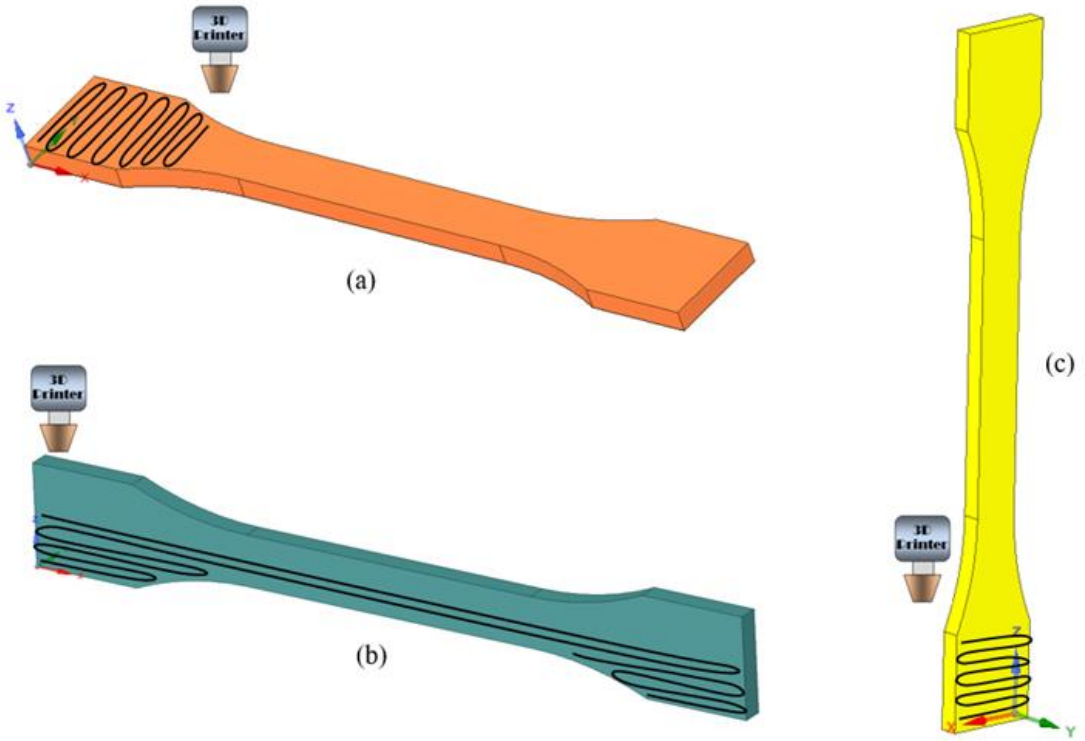

Fig. 5.1 The main directions for 3D printing the specimens: (a) horizontal specimen (in the XY plane), b) lateral specimen (in the XZ plane), c) vertical specimen (in the XZ plane)

To allow an easier identification of the type of specimen, the following notations were used: XY specimens – for those manufactured in the horizontal plane (fig. 5.1(a)), XZ1 specimens – for those manufactured in the lateral plane (fig. 5.1(b)) and XZ2 specimens for those extruded in the vertical plane (fig. 5.1(c)).

A. Evaluation of the mechanical response under the action of tensile forces for XY specimens manufactured in the horizontal plane

The first four specimens were built on the horizontal base of the 3D printer, positioned according to figure 5.1 (a). This orientation allows a satisfactory definition of the external profile of the part, given the easy positioning. The determination of the mechanical characteristics will be carried out using the INSTRON 8872 system and the digital strain gauge.

The stress-strain graph shows that the specimens XY-3 and XY-4 have a higher tensile strength compared to XY-1 and XY-2, the failure of the material occurring at a specific strain of more than 3%. The variation, in terms of maximum specific strains, is due to the dispersion

of the carbon microfibers within the thermoplastic filament, which results in increased performance or decreased performance, depending on the alignment of the microfibers with the direction of pull.

The main characteristic of this orientation, which results from the measurements carried out, is the high degree of elasticity. The average specific elongation supported by the tested samples is approximately 1.85%, which indicates a satisfactory elastic behavior of the extruded material in this direction.

The experimental results highlighted the achievement of tensile mechanical properties relatively similar to the XY specimens extruded in the horizontal plane. With an average tensile strength of 47.29 MPa, these specimens are 50% stronger than vertically fabricated specimens and 5.15% stronger than horizontally printed specimens. The specific stress-strain curve shows a slight decrease in stress after passing the point corresponding to the maximum stress, followed by material failure.

The mechanical characteristics obtained from the tensile tests for this specimen type exhibit high accuracy, thanks to the very low coefficient of variation, below the value of 5%. Compared to the values provided by the manufacturer through the technical sheet of the CPE CF112 Carbon filament, the results are similar to those obtained for the XZ1 printing direction, thus providing a similar mechanical behavior in the two manufacturing directions. The central section has an approximately constant area of 10 mm x 4 mm. The necking phenomenon was not observed in any of the extruded specimens tested in tension.

The obtained results can be considered correct in view of the fact that material breakage occurs, most frequently, in the central section of the tensile specimens. The lack of a necking is a confirmation of the fact that the composite material has a reduced ductility, being rather characterized by a brittle behavior.

B. Evaluation of the mechanical response under the action of tensile forces for XZ1 specimens manufactured in the lateral plane

The 3D printing on the side of the specimens was done using support brackets, to preserve the geometry of the specimen and to match the orientation in figure 5.1 (b).

It resulted in a similar evolution of the specific stress-strain graph on the 0.05% - 0.15% segment, for all four studied specimens. This fact is due to a constant density of material in the body of the specimen, in correlation with the modulus of elasticity, whose average value is 4783.22 MPa, having a very small variation of only 0.65%. Compared to XY and XZ2 type specimens, this type of specimens has the highest modulus of elasticity.

The yield stress corresponding to a plastic strain of 0.2% has an average value of about 38.86 MPa. The importance of this parameter lies in the fact that it is frequently used by manufacturers of engineering materials to characterize the mechanical behavior of the material.

The fracture occurred through an approximately horizontal section of the material at an average stress value of 44.97 MPa, showing a relatively small standard deviation of 1.87 MPa. The low value of the deviation confirms that the material has an almost constant mechanical behavior, as well as the fact that there are no factors involved in the manufacturing process that could cause inconstant values.

The coefficient of variation has a value below 5%, for all the experimental tests performed and for all the reference parameters measured, indicating a high degree of accuracy of the tests. The practical justification is the quality of the thermoplastic extrusion process, a process that produces similar components in tems of finishing.

By comparing the results with the data provided by the manufacturer, it can be seen that the samples manufactured in this direction have double the modulus of elasticity than that presented by the manufacturer. On the other hand, the average value of the flow limit is 34% lower compared to the data shown in the technical sheet. Given the low standard deviation and coefficient of variation, the obtained results can be considered to be within the acceptability limit.

The failure of the material occurred suddenly, in the vicinity of the central section, in the case of some specimens and towards the ends in the case of other specimens. Due to the fact that they are printed with the extruded filament in the tensile test direction of the material, the material will have superior properties in the XY and XZ1 directions, having a continuous character, compared to the XZ2 printing direction.

Given that this printing direction provides the highest modulus of elasticity, it can be deduced that structures fabricated in this manner will better retain their initial geometric characteristics under the prolonged effect of external stresses.

C. Evaluation of the mechanical response under the action of tensile forces for the XZ2 specimens printed in the vertical plane

The tensile tests realized in vertical direction, according to figure 5.1 (c), constitute the last addressed printing direction. Taking into account the way the layers of material are overlapped, the failure section will be located in the area of adhesion between the layers of extruded filament, due to the weak intermolecular bonds between the layers of the chlorinated polyethylene elastomer. Thus, carbon microfibers play a less important role in the strength of the material, due to the fact that they cannot take the load.

After the stress threshold of 31.50 MPa, the specimens break by detaching the material layers, in the section where the adhesion between the layers is the weakest. In the context of the absence of manufacturing defects, material failure occurs when the tensile force exceeds the adhesive force of the material. However, manufacturing errors, such as incomplete ripening, temperature variations or the appearance of porosities, can diminish the performance of the material and represent the triggering factor for breakage.

The yield strength corresponding to a plastic strain of 0.2% is about 29.56 MPa, the average tensile strength is 31.50 MPa, while the specific strain of the specimens is lower compared to the previous printing directions. Compared to the previous specimens tested in tension, the rupture occurs much faster, with the two sections of the material separating completely. It can be noted the predominantly linear evolution of the specific stress-strain curve, compared to the previous tensile tests. The reduced performance of the XY2 specimens is confirmed by the average value of the longitudinal modulus of elasticity, being 29.62% lower than the specimens manufactured in the lateral plane and 33.62% lower than in the case of the specimens manufactured in the horizontal plane.

The coefficient of variation has a value below 1.40%, for the first three elastic mechanical characteristics determined, while the specific strain has a variation of 6.53%. This aspect may be the result of the difference in the ripening time of each sample, the first sample having a longer time allocated for material uniformity while the last one had a shorter time, all being taken simultaneously from inside the manufacturing device. The relatively small variations provide a high degree of confidence in the precision of the experimental results.

In relation to the data provided by the manufacturer, the mechanical characteristics are generally weaker, with the exception of the modulus of elasticity, which has similar values. Compared to the previously studied specimens, this orientation provides significantly lower performance. Thus, within the composite blade, orientation of the manufacturing direction perpendicular to the traction direction will be avoided.

D. Evaluation of tensile tests using the DIC method

In order to obtain a set of measurements as accurate and as relevant as possible for the studied materials, one sample type of each three previously presented orientations was subjected to the same tensile stresse, the mechanical characteristics being assesed with the digital imaging process (DIC). In this way, a comparative evaluation of the two methods of measuring material characteristics can be made.

Comparing the data obtained from the digital extensometer with the results determined using digital imaging correlation revealed a minor difference in material deformation, this being more a characteristic of the specimen and not of the measurement method used. The evolution

of the specific stress-strain curves fits, in general, the previous tests performed for each type of specimen.

The mechanical characteristics measured using the DIC system have similar values to those evaluated using the load-cell of the Instron equipement, with no notable differences in the measured values. Thus, it can be concluded that the evaluation methods have a similar level of precision, the current data set can be used to determine the average values required in the numerical simulations.

E. Evaluation of the mechanical response under the action of compressive stresses. Comparative analysis between CPE and 5052 aluminum alloy

The mechanical properties of ductile materials are almost identical in tensile and compressive tests. However, the results are different for brittle materials such as fiber-reinforced composites, thus both types of tests are needed to obtain a complete characterization of the mechanical properties.

The compression characteristics of the honeycomb structure were determined using the INSTRON 8872 experimental test system, equipped with test type specific adapters. The experimental compression test was carried out for 12 cubic specimens, with hexagonal cells, four of which were manufactured by thermoplastic extrusion of CPE filament reinforced with carbon microfibers, and eight were made of aluminum, according to NIDA specifications 2.3-3/8- .0015 P(5052).

The stresses and strains for the compression test of both materials were determined using the digital image correlation system, with the specimens previously painted in contrasting colors to facilitate the system's evaluation.

The applied force has an approximately linear evolution for all four specimens subjected to compression stresses. Its maximum is reached in the range 1.2892÷1.4065 kN, resulting in an average actuation force of approximately 1.3614 kN.

The maximum displacement achieved during compression has similar values for all samples, being located close to the threshold of 1.30 mm. Compared to the height of the honeycomb structure of 80 mm, after material failure was attained, the specimen was compressed by approximately 1.625% of the initial height.

The approximately linear variation of the graph represents the effect of the uniform application of the compression force, corresponding to a value of 2 mm/minute, respectively 0.0325 mm/second. The failure condition of the specimens occurred after approximately 38 seconds, under the action of compressive stresses.

The mechanical behavior of the studied samples is similar for all four experimental tests. The slope of the specific stress-strain curve is relatively identical throughout the tests. The minimum equivalent stress was identified in specimen number 3, having the value of 1.2567 MPa, corresponding to a specific strain of approximately 30.89 %. In contrast, the maximum breaking strength corresponds to specimen number 4, with a value of 1.4617 MPa at an equivalent strain of 31.47%.

Material yielding during compressive stress is characterized by the occurrence of delamination between layers of extruded material. The stiffness of the material has the effect of moving the layers of material in the lateral directions, thus leading to the deformation of the hexagonal cells of the honeycombs. The significant character of the delaminations is most visible on the free sides of the honeycomb, where the structure has the lowest level of consolidation. Actual rupture of the extruded material cords was not identified on the specimens. The deformation of the material had a progressive character, directly proportional to the applied compression force, no specific point of failure of the material being identified. The specimens have been previously painted in contrasting colors to facilitate the system's measurements.

The average value of the modulus of elasticity to compression, resulting from the experimental tests, is higher than the value of 2200 MPa presented in the technical data sheet

of the material. This difference denotes that the material performs better in compression than in tension, thus being suitable for use as a central core inside the anti-torque blade.

In contrast, the average normal stress in compression represents 83% of the value presented by the manufacturer for the tensile test, at the time of failure of the material. This tension reaches higher values under tensile stress due to the carbon microfibers dispersed in the material and oriented in the direction of loading.

The compression test of the 5052 aluminum alloy honeycombs was performed under the same conditions as the compression test of the thermoplastic extruded material. Eight honeycomb specimens were extracted from a NIDA 2.3-3/8-.0015 P(5052) panel to determine mechanical properties under compression.

Their total size was measured so that the total surface on which the compressive force is applied by the load-cell is comparable to that of the honeycomb specimens.

Considering that the coefficient of variation is only 8.26%, it can be deduced that the NIDA honeycomb aluminum alloy has a relatively constant mechanical behavior.

From the analysis of the results obtained for the two types of materials subjected to the analysis, the following aspects can be stated:

- the aluminum alloy allows the achievement of a higher compressive force in the linear-elastic range of the material, in a significantly shorter time interval, compared to the extruded polymer, under the conditions of an identical stress. This aspect denotes a faster loading as well as a faster failure of this material;

- the stress-strain curve of the thermoplastic extruded filament shows a constant evolution with the increase of the applied stresses, the breaking of the material occurring at a deformation much higher than the aluminum alloy;

- given the densities of the two materials, it can be concluded that the thermoplastic polymer reduces the total mass of the honeycomb core by approximately 34.1% compared to the aluminum alloy; also other improvements induced by this modification are chemical resistance, corrosion resistance, as well as resistance to prolonged stress.

Considering the nature of the stresses as well as the aeroelastic behavior of aircraft structures, it can be concluded that the carbon microfiber reinforced chlorinated polyethylene filament is a good substitute for NIDA honeycombs made of aluminum alloy 5052, offering good performance for use as a honeycomb core in the tail rotor blade, made of composite materials.

5.3 Determining the mechanical characteristics of the material used to manufacte the spar of the blade

The blade spar represents the main strength structure embedded inside the blade, being comprised of the laminated composite shell and the honeycomb obtained by thermoplastic extrusion, along approximately its entire length.

This structure is made of carbon roving, representing the grouping of carbon fiber filaments, parallel to each other, held together by means of an adhesive. The manufacture of rovings is done manually by progressively joining carbon filaments with epoxy resin.

Given the positioning of the carbon fibers on the longitudinal axis of the spar, their bearing capacity is maximum, the stretching of the fibers due to centrifugal force and aerodynamic stresses taking place in this direction.

The mechanical behaviour of the material was studied experimentally by means of tensile testing. These tests were performed on the INSTRON 8872 uniaxial testing system, for a total of five dog-bone specimens. The test system measures, by means of the built-in transducers, the values of the applied force, of the displacement, as well as the duration of the tests.

The specific stress-strain graph reveals a similar evolution for all samples made of carbon roving, for the range of specific strains 0.01% – 0.7%. The determination of the modulus of elasticity, as the slope of the stress-strain curve, was carried out for the range of strains 0.01% - 0.5%, resulting in an average value of 65.839 GPa. The average breaking strength determined at the moment before the failure of the material has a value of 587.77 MPa and manifests itself by breaking the matrix and by the appearance of delamination.

The specific stress-strain curve has a bilinear elastic character for all the specimens tested in tension, the most visible aspect for specimens no. 2, 4 and 5.

The sixth specimen of this type was used for a preliminary test to establish the test conditions and the ability of the system to break the chosen material. The time required to reach breaking strength varies between 65÷100.6 seconds, the average being 79.82 seconds.

The yielding of the material occurs at different specific deformations, varying in a range of values between 0.86% ÷ 1.42%. The results obtained are lower, compared to the resistance values of the fibers offered by the manufacturer. Taking into account this aspect and the fact that fiber breakage could not be visually identified, it follows that the failure of the composite material is the result of the epoxy resin matrix breaking, manifested locally by the appearance of delamination of the material layers.

5.4 Determining the mechanical characteristics of the material used to manufacture the skin of the blade

The skin is the structure that encloses the main resistance components, giving the anti-torque blade its strength and aerodynamic shape. It is made of a multi-layered composite material, which is based on the following materials:

- 2/2 twill carbon fiber fabric, which provides a high level of strength, offering equal tensile performance in both the weft and warp directions.
- The epoxy resin used as an adhesive is the most suitable for the realization of composite materials reinforced with carbon fibers, because it ensures a very good adhesion, offering, at the same time, a very good strength-to-mass ratio.

The tensile specimens were made from 12 sheets of carbon fiber fabric, bonded with epoxy resin, resulting in a total specimen thickness of approximately 3.96 cm. The skin of the composite blade was made from a number of three overlapping laminae, thus resulting in a unitary laminated composite material with a thickness of approximately 1 mm.

A. Evaluation of the mechanical tensile behavior of the material made from a single laminate

By studying a single composite sheet, it is possible to analyze the characteristics of the deformations and stresses that appear at the level of the elementary components of a carbon fiber fabric (weft and warp), arranged perpendicular to each other. The Istra 4D image processing program was programmed to capture up to 500 frames at the time of the experimental trial at a frequency of 5Hz.

The ends of the unilaminar specimens were reinforced by gluing with a strong adhesive some aluminum segments on both sides of the specimen, so as to avoid the ovalization of the clamping holes (found in the preliminary tests) and to allow the proper loading of the composite.

The 2/2 twill fabric uses 3K type carbon fibers in two weft directions and two warp directions, thus resulting in the visual effect of diagonal lines. Due to the high number of fibers used, the fabric has an opaque character, consistent thickness and high durability.

A total of ten specimens were used for this type of experimental test, five of which were cut along the weft of the warp (marked with the letter "U" in the previous figure), and the other five were cut along the weft (marked with the letter "B").

The experimental tests were carried out in order to determine the mechanical characteristics of the material (Young's mode and Poisson's ratio). Given the high strength of

the fabric, as well as the low power of the traction motor, it was not possible to achieve the breaking strength of the material. The maximum tensile force applied to the specimens is in the range of 493-602 N.

The average value of the longitudinal modulus of elasticity is 23585.49 MPa, relatively similar to the average value of the specimens cut in the warp direction, while the Poisson's ratio has an average value of 0.3495. Due to the relatively high value of Poisson's ratio specimen B1 compared to the rest of the tests, it was not used to determine the average values previously specified.

The proximity of the values obtained for the two types of samples confirms that the material can be considered isotropic in two directions. Thus, an average value for the mechanical properties of a single lamina can be estimated, which will form the basis of future numerical simulations.

The stress-strain graph reveals a similar variation for all five studied specimens, the major difference being in the case of specimen U2, whose linear-elastic variations are much lower than the general average. Due to the aluminum reinforcement of the ends of the specimens, it can be deduced that the variation of the specific stress-strain curve is irregular during the first portion of the stress, until the proper tensioning of the material is achieved.

Relative to the applied force, of approximately 500 N, the maximum stresses resulting from the experimental tests are around 120 MPa. Considering the characteristics of the two base materials, this value is sufficient to break or crack the hardened epoxy resin, but it is far too small to exceed the yield strength of the carbon fiber fabric.

In order to study the microscopic behavior of the tensile specimens, several sequences from the Istra 4 D program were presented. The displacements in the Z direction (perpendicular to the plane of the specimens) are determined by the analysis program with the elimination of rigid body motion (RMBR - Rigid Body Movement Removed), for a more precise visualization of the movement of the fibers in the fabric composition (5.2). We can see the weft tensioning of the two samples, which are positioned along the entire length of the material. The maximum displacement is highlighted by the red color, being the weft fibers, which retreat to the horizontal plane of the material, while the warp fibers remain in a more relaxed posture. The displacement of the carbon fibers produces the effect of diagonal lines, given the 2/2 twill construction of the fabric. The similar effect is shown in the case of deformations, for the specimens having the warp in the tensile direction, with the mention that the diagonal directions that reflect the tension are positioned in the mirror to the previous set of specimens.

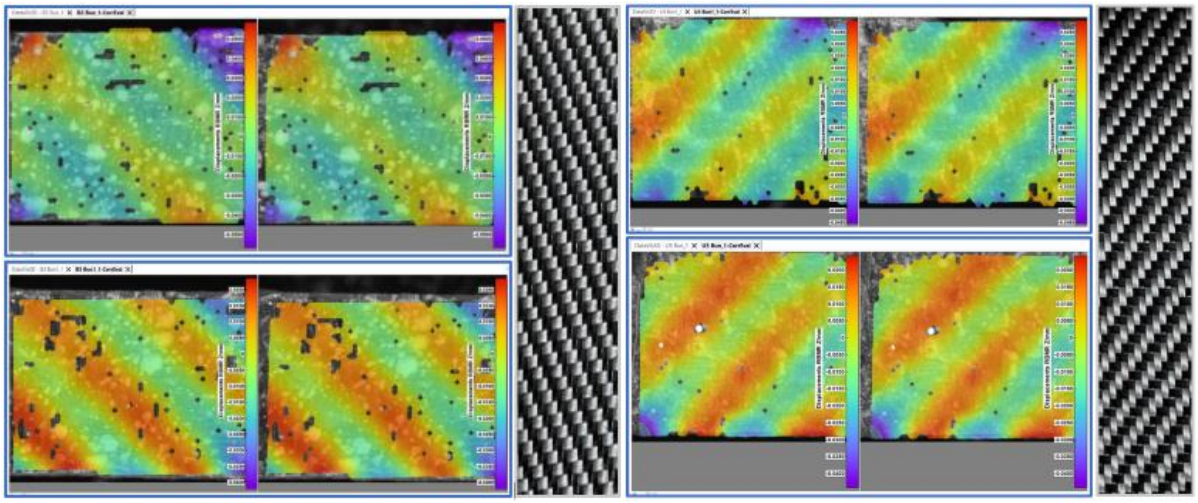

Fig. 5.2 Displacements on Z direction for the specimens B_2, B_5 și U_4, U_5

The specific material deformations shows a similar distribution of the color codes, highlighting the presence of maximum values on the fabric components, where the stress is at its peak. On the right side of the figures, the positioning of the 2/2 carbon fiber twill fabric can be seen, from which the correspondence of the maximum values in the program with the way the fabric is joined can be seen.

The segments in the figures that are not colored indicate the discretization nodes that could not be followed by the software program during the experimental trials, without changing the overall effect on the material, which remains clearly visible.

Movements of the material in the Z direction are an indicator of its retraction towards the horizontal plane of symmetry, reducing the thickness of the material to the extent of progressive stiffening. Within a multi-layered laminated composite, the observed local effect can lead to the occurrence of delamination between adjacent material layers, due to the weakening of the adhesion of the epoxy resin.

B. Evaluation of the mechanical behavior, under the action of stretching forces, of the multilayer laminated composite

The material used to make the blade sheath is a laminated composite, made of carbon fabric and epoxy resin, offering a much higher tensile strength than thermoplastic extruded filament. A total of five dumbbell ("dog-bone") specimens were used, four being characterized according to the data provided by the force cell of the equipment, and the last one was studied using the DIC Q400 system. Such laminated composites are frequently used in aeronautical applications, where structural loads are very high.

Fiber breakage was almost non-existent, mainly due to the fact that the breaking strength of the carbon fabric (declared by the manufacturer in the data sheet) is about ten times higher than the average breaking strength, measured experimentally on the investigated specimens.

The specific stress-strain diagram resulting from the variation of the applied force with the resulting displacement, allows the determination of the main material characteristics, such as the modulus of elasticity or the breaking stress. Given the bilinear elastic behavior of the material, the modulus of elasticity was determined for two reference intervals from the graphic evolution, respectively 0.05÷0.15% and 1.1÷1.3%.

The values of the main mechanical strength characteristics are below those of the previously tested carbon fiber roving, given the fact that the fibers are oriented in two directions. The value of the standard deviation is below 5% for most of the tests evaluated using the load cell, which results in a high level of accuracy of the tests performed.

The values presented above are close, in order of magnitude, to the data provided by the material manufacturer. The average strain in the data sheet is about 1.3%, compared to the average of 1.42% obtained experimentally, and the average breaking strength of 480.57 MPa is about one third of the value of 1.86 GPa shown in the data sheet. The differences found are most likely due to different testing methodologies for the laminated composite, given that the epoxy resin and the fabric are produced by different companies that used different test standards.

The main advantage of using the non-contact DIC imaging system is the possibility of determining the transverse contraction coefficient of the material, without the need for additional devices. Thus, the Poisson's ratio value of 0.353 for the laminated composite material resulted, very close to the average value obtained for the unilaminar material.

Due to the high tensile stresses, the adhesion between the fabric and the resin gradually decreases until it fails, resulting in the separation of the laminae along the entire central portion, parallel to the carbon fibers.

The practical advantage of this type of material is that it is not characterized by a sudden break, being able to ensure the temporary operation of a helicopter component until the moment of safe landing (depending on the severity of the damage).

C. Evaluating the mechanical characteristics of the material subjected to three-point bending

The varied aerodynamic demands during helicopter flight determine the need to develop a material that has good resistance to the bending moment developed at the free end of the blade by aerodynamic forces. The blade skin is the second element in length, after the strength spar, which must exhibit reasonable aeroelasticity.

Bending is the result of transverse loads, which produce both bending moment, manifested by normal stresses linearly distributed over the height of the blade section, and shear force, which produces zero tangential stresses at the extremities and maximum at the center of the section.

Three-point bending is a commonly used method for testing materials loaded with a bending moment, and can be performed to either ASTM or ISO standards to ensure test reproducibility and the most efficient characterization of material properties.

A layer of white paint was applied to the surface of interest of the samples, according to the methodology previously described for the measurements made with the digital image correlation system. Fine particles of black paint were sprayed over the white layer, so as to create the necessary contrasting points, which the DIC system will follow in order to evaluate the deformations produced.

The deformations in the longitudinal plane of the specimens subjected to bending are characterized by the stretching of the lower fibers of the fabric and the compression of the upper fibers, the two sections being separated by a neutral plane, where, theoretically, the longitudinal deformation is zero. In practice, the longitudinal deformations are also accompanied by transverse contractions, so that in the stretched area the thickness of the bar decreases, and in the compressed area the thickness of the bar increases, according to the phenomenon of anticlastic curvature.

Figure 5.3 shows two sequences from the Istra 4D program, in which the incipient phase of the bending stress is captured (a), as well as the final sequence, in which the rupture of the material is visible (b).

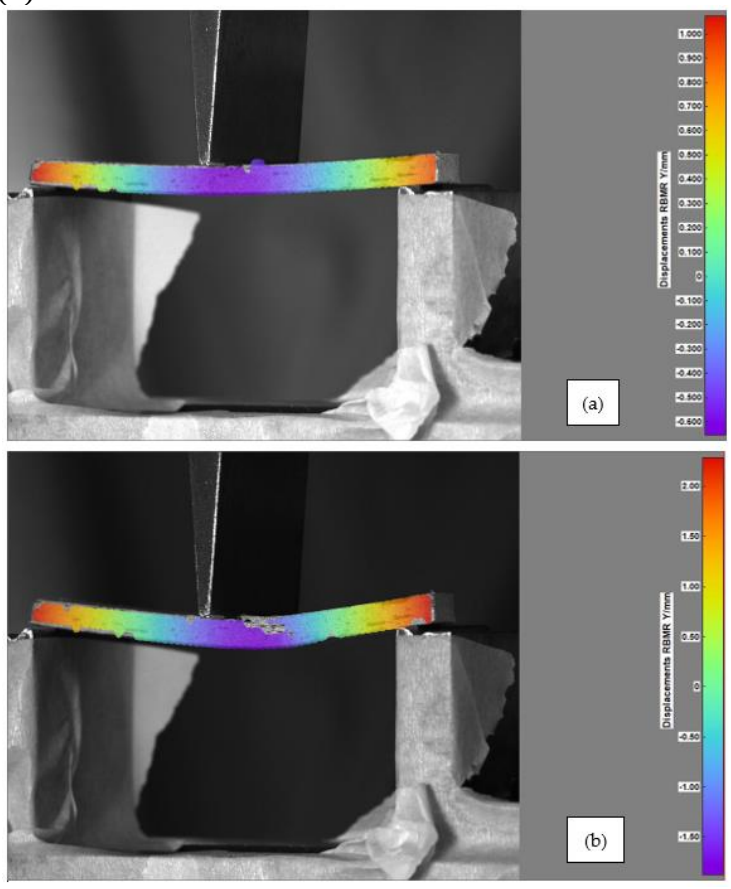

Fig. 5.3 Phases during three-point bending tests, from the Istra 4D software

The tearing of the material is visible in the area where the color spectrum of the software program disappears. The variation on the linearly elastic portion is similar for all three specimens. The evolution of the elastic linear segment of the graphs is similar up to the maximum stress value recorded during the tests, of 0.5966 kN. The first two specimens are characterized by a constant level of deformation, after reaching the maximum stress, while the third specimen records a decline, followed by material failure.

The average maximum stress felt by the material during the experimental test has the value of 311.47 MPa, being followed by a linear plasticity level decreasing, according to the graphic evolution. The specific strain of the material has the average maximum value of 0.7988 %. These data will serve for comparative purposes, for the validation of future numerical analyzes carried out with the finite element method.

The tests carried out led to the determination of an average modulus of elasticity of 92.212 GPa. The maximum force used to stress the specimens in bending was 590 N, resulting in a maximum recorded displacement of 1.34 mm.

5.5 Conclusions

The experimental tests carried out in traction, compression and bending took into account the specifics of the operational demand of each structural component of the anti-torque blade.

The determination of the material properties for the honeycomb core of the future composite blade was carried out by means of experimental tensile and compression tests. The elastomer selected for this structure is made of chlorinated polyethylene, reinforced with carbon microfibers CPE CF112 Carbon, a material with very good mass and resistance characteristics, desirable for aeronautical structures.

The tensile test of the material was carried out on a number of 15 3D printed samples, five for each of the three manufacturing directions, in order to evaluate the orthotropic character of the material. The experimental results reveal a similar mechanical behavior for the XY and XZ1 manufacturing directions (built in the horizontal and lateral planes, respectively), given the close values of the tensile strength, yield strength and elastic moduli, with a slight difference in favor of the XY specimens. In contrast, specimens made in the vertical plane (XZ2) show markedly inferior characteristics, up to 50% weaker than previous printing directions, which is why they are not viable for tensile stress.

The material skin is the thin-walled rigid structure that provides the blade with both aerodynamic and strength characteristics to withstand the various stresses encountered in helicopter operation.

Made as a laminated composite of 3K GG 285 T carbon fiber fabric and Derakane Momentum 470-300 epoxy resin, the material was subjected to tensile and three-point bending tests to determine the material characteristics essential for a characterization as complete and as faithful as possible.

Laminate tensile testing was initially performed on unilaminar specimens, placed under the digital microscope, and the results were then correlated on a larger scale with multilaminar composite specimens.

Determining the experimental results is essential for performing finite element analyses, at which point the geometrically modeled structure will be subjected to similar flight conditions to determine its effectiveness from a practical point of view.

6. Reproducing the previously presented material tests as finite element analysis. Comparative validation of the results

The experimental tests represent a fundamental phase for determining the mechanical characteristics of the components used in the manufacture of the anti-torque blade. Given this aspect, several numerical analyzes were carried out, the results of which will be compared with the experimental tests, for each type of material.

The finite element analysis carried out in the ANSYS Workbench, was aimed to reproduce as faithfully as possible the test conditions of the materials. The geometric models of the samples were made using the average values of the dimensions of the samples tested experimentally.

The aim was to obtain the following results, which will form the basis of the comparative validation:

- the maximum values of the von Mises equivalent stress;
- maximum deformation values;
- the reaction force at the point of embedding the samples.

Through the process of validating the static analyses, specific to each material, it will be possible to determine the average error for each type of request, the level of simultaneity of the numerical analyzes compared to the experimental tests, thus constituting the foundation of the numerical modeling and analysis of the composite blade as a whole. The basis for the comparative validation is the average of the experimentally measured data, with real values being used for stresses and strains.

6.1 Finite element analysis of the compression tests

Compression testing of CPE CF112 Carbon extruded filament honeycomb specimens was performed on the same geometric CAD model used in 3D printing, thus ensuring an accurate correlation between the physical and designed model.

The specimen was fixed on the lower surface of the hexagonal cells, and the maximum vertical displacement obtained during the experimental tests, of 1.3489 mm, was applied to the outer surface, as the average maximum displacement of the four specimens with hexagonal cells subjected to compression.

By applying the maximum displacement to the upper surface, the reaction force measured in the lower fixed surface can be determined. The obtained reaction force has the value of 15251 N, being 17.8% higher than the value measured by the force cell of the Instron system, respectively 12936 N. The main results obtained from the static analysis for the honeycomb specimen are presented in figure 6.1.

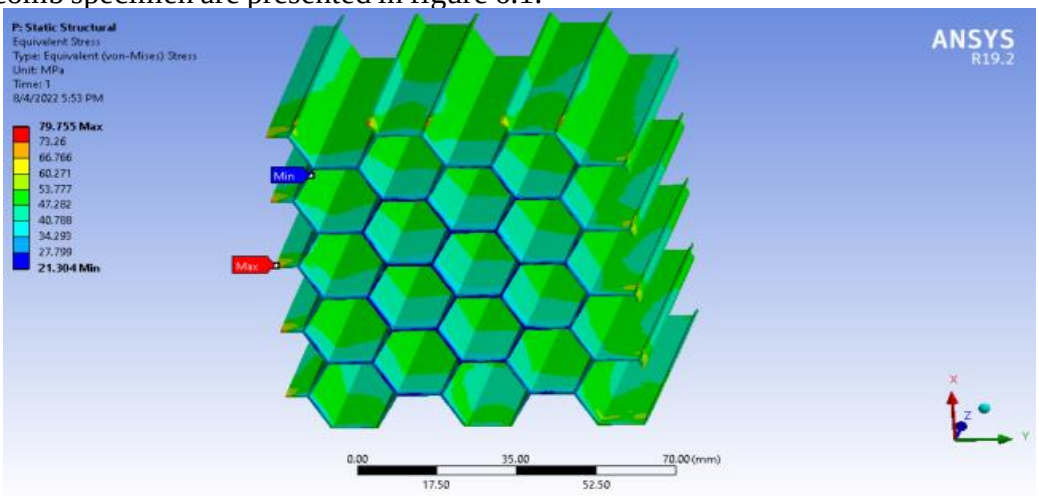

Fig. 6.1 Distribution of equivalent von Mises stresses on the body of the specimen

The maximum equivalent stress resulting from the numerical analysis has the value of 79.75 MPa, which is approximately 12.77% higher than the experimentally determined value of 70.71 MPa. The location of the maximum and minimum stresses in the lower section of the specimen is consistent with the real visible effect, being similar to a veiling phenomenon of the hexagonal cell walls.

The maximum strain has a similar manifestation to the maximum equivalent stress distribution in terms of its location. The alternating color zones on the walls of the hexagonal cells are specific to a veiling phenomenon, characterized by the lateral movement of superimposed layers of extruded material.

The results obtained through the numerical analysis reveal a satisfactory similarity for the main mechanical characteristics of the studied material, with an overall error of less than 15% in relation to the experimental values. Given the agreement of the numerical simulation results with the experimental data and with the data provided by the manufacturer in terms of material characteristics and mechanical behavior, it can be concluded that the results are appropriate and can be used in future numerical analyzes to study the performance of the composite blade.

6.2 Finite elements analysis of the tensile test

A. Static structural analysis of the carbon fiber reinforced material

The composite blade skin, made of a fiber-reinforced composite material, based on a polymer matrix of epoxy resin and 2/2 twill fabric of carbon fibers oriented at 0°/90°, is the structural element of the blade subjected mainly to tensile traction during helicopter flight.

When tested, the composite material subjected showed a bilinear evolution of the specific stress-strain curve, an aspect that was taken into account when defining the material properties of the numerical model.

By applying the maximum displacement of 1.7926 mm, as the average of the maximum displacements of all the tensile tested specimens, a reaction force in the fixed surface of the specimen of 24.528 kN resulted, approximately 8% higher than that measured by the load cell. The values of the most important performance indicators of the stress distribuition is presented in figure 6.2, for the specimen subjected to the tensile test.

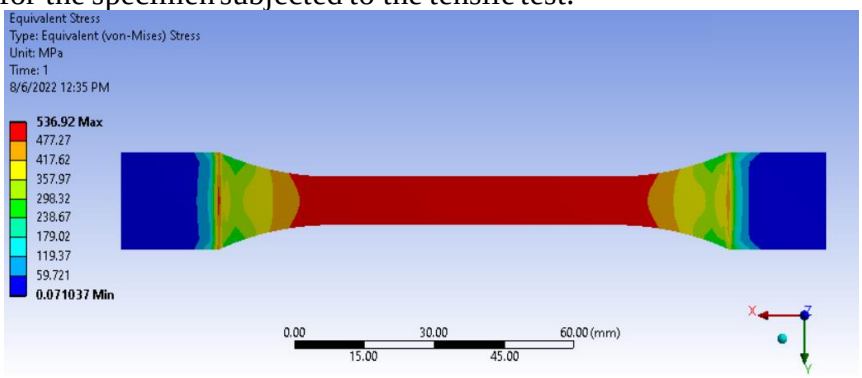

Fig. 6.2 Distribution of maximum stresses on the body of the laminated composite specimen

Considering the way the specimens are constrained, it can be stated that the maximum tension is felt in the central area, as well as in the vicinity of the passage from the foot of the specimens to the necked area, reaching the maximum value of 536.92 MPa. The largest deformation occurs in the central section and has values similar to those determined experimentally.

The static analysis was performed using two main approaches. In the first case, the dumbbell specimen was made in the form of a solid geometric model, and in the second case, the ACP module of the Ansys program was used to define the material properties for a single

laminate, according to the tensile test results for the unilaminar samples, the characteristics of the laminated composite material being later defined (number of laminae, orientation, arrangement method, etc.).

The results reflect a greater convergence with respect to the simulation performed for the solid geometric model, given the fact that a larger set of experimental data was available for material characterization compared to single-laminar tensile tests. The latter were made using a low capacity traction device, which could not reach a force high enough to break the material, the material characterization data being therefore relatively brief.

The average error for the solid-based numerical simulation has values below 10% for all parameters of interest, while the unilaminar material characterization resulted in differences between 10-15% for all parameters of interest.

The results of the numerical analysis indicate an acceptable approach for the main parameters of interest of the comparative validation. Given the fact that the material is a composite one, with a polymer matrix on the one hand and reinforcing fibers on the other, its mechanical characteristics are located, both from an experimental point of view and from the point of view of numerical analyses, between the properties of the constituent materials. Thus, the breaking strength of the laminated composite material is 484.495 MPa, above the value of 85 MPa of epoxy resin and below the value of 4410 MPa of carbon fiber fabric. Given the relatively close correspondence of the numerical results with the experimental measurements, the credibility of the data can be supported, as well as the possibility of using them in numerical analyzes to determine the performance of the anti-torque blade.

B. Static structural analysis of the carbon fiber roving test

The spar of the anti-torque blade is the most important resistance element of the anti-torque blade. Its positioning along the entire length of the blade, as well as the presence of mounting holes at its base, lead to the need for very good performance characteristics. Given this fact, it was decided to manufacture it from unidirectional carbon fibers (roving) with superior tensile strength properties.

The characteristic curve of the material, determined by the practical tensile test, presents a bilinear evolution, with a linearly elastic portion and a linearly plastic portion, each having its own longitudinal modulus of elasticity.

The geometric model of the dumbbell specimen is clamped at one end, while the experimentally determined maximum average force is applied to the other end to determine the maximum displacement and stress and strain values.

Figure 6.3 shows the obtained stress distribution for the tensile test of the carbon roving sample, when applying a force of 2307.43 kgf, respectively 22628.12 N.

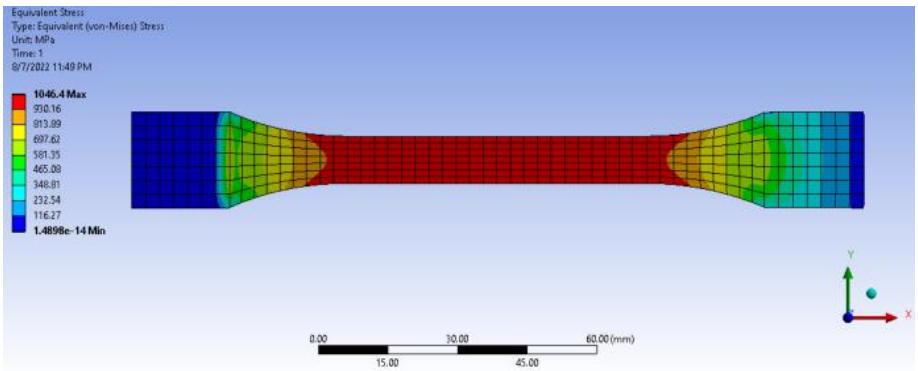

Fig. 6.4 Distribution of equivalent von Mises stresses on the body of the carbon roving specimen

The static analysis resulted in a maximum displacement of 1.3876 mm, only 4.5% higher than the measured experimental value. The maximum equivalent stress and the maximum

specific strain occur on the central area of the tensile specimen, with differences of up to 20% compared to the experimental measurements.

The comparison of the previous results indicates a satisfactory correspondence between the results of the numerical analysis and the experimental results, considering that the experimental data is actually an average of the five specimens tested in tension. According to the technical data provided by the manufacturer Torayca, the fibers have a breaking strength of 3530 MPa, and the composite material reinforced with these fibers has a tensile strength of 1860 MPa, a value relatively close to the experimental result.

6.3 Finite element analysis of the three-point bending test

Given the relatively long length of the tail rotor blade skin, which represents a flexible aeroelastic structure, it is of interest to know the properties of the material of manufacture in case of bending stress.

Three-point bending is the easiest way to determine the mechanical characteristics, given the fact that the phenomenon is local and easy to put into practice.

The finite element analysis of the bending phenomenon was carried out, similar to the tensile stress, both in the case of the solid geometric model and in the case of the laminar model, defining all the characteristics of the composite material. The laminar model defined using the ACP module respects the real characteristics of the composite, being made of 10 overlapping laminae, keeping the same orientation throughout its layout.

In order to reproduce the experimental test conditions, within the finite element software, the geometric model was constrained near one of the extremities (on the lower edge), and at the opposite end all freedoms of movement were restricted, except for movement along the axis longitudinal of the specimen.

The average maximum displacement determined experimentally, with the value of 1.351 mm, was applied to the central section of the specimen, according to figure 6.5, where its undeformed contour can also be observed. In order to capture the occurrence of local effects, within the software program it was decided to use 30 sub-steps for calculating the results.

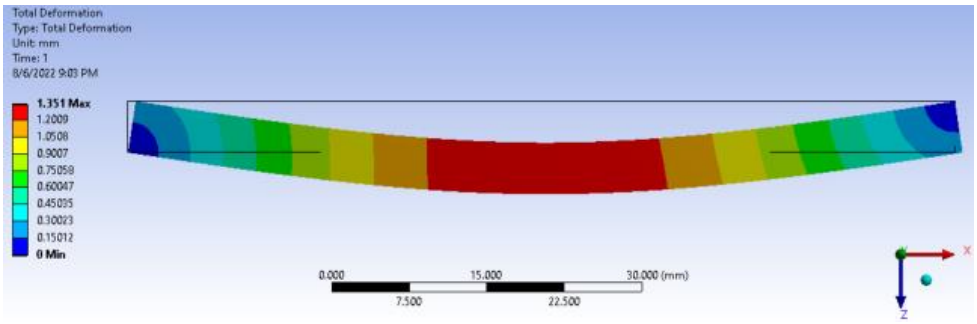

Fig. 6.5 Maximum displacement of the specimen subjected to bending

The maximum specific deformation of the rectangular specimen occurs on its upper surface, at the central point of application of the external force, reaching the maximum value of 0.741%. The stress distribution indicates how the top surface compresses, the inner surface stretches, and the middle fiber exhibits the lowest strains.

The agreement with the experimental data is shown by the acceptable error value of about 13% for the equivalent stresses and only 6.89% for the reaction force, measured at the point of embedment of the specimen.

Considering the results of the numerical analyzes carried out both for the solid model and for the laminar composite model, the validity of the obtained results in relation to the experimental data can be concluded. This aspect is supported by the fact that most of the

numerical analysis results fall between the minimum and maximum values of the set of experimental trials. Also, with regard to the technical data provided by the manufacturers, the numerical results lie, similarly to the tensile analysis, between the specific performance values for the epoxy resin, on the one hand, and the performance values of the carbon fabric, on the other part.

6.4 Conclusions

Testing the materials at the basic stresses present during normal operation is an essential condition for determining their breaking and deformation limits, information that is the basis of finite element analyses, necessary to evaluate the anti-torque blade performance. To strengthen the confidence in the complex static analyses of the composite blade, a correlation of the experimental data with the results of the numerical analyzes was first carried out to reproduce the experimental tensile, compressive and bending stresses.

The numerical analyzes carried out had values close to the experimental results, with a maximum error below 15% for most of the cases addressed, thus being appropriate to correlate to the tail rotor blade performance evaluation, under flight-like conditions.

7. Composite tail rotor blade - manufacturing and experimental tryouts. Validation of the finite elements analysis results

7.1 Manufacturing process of the composite tail rotor blade

The manufacture of the tail rotor blade from composite materials, at a scale of 1:3 in relation to the real dimensions of the metal blade, was realized manually, by the "hand lay-up" method, from the same composite materials subjected to the previously presented experimental tests. The manual manufacturing of composites is the classic production method, which involves following successive stages and is based on the practical experience of the one who performs the operation. The main stages that have been completed in order to manufacture the composite blade are the following:

a) Construction of a provisional model of the anti-torque blade at 1:3 scale from a malleable resin;
b) Defining the separation plan of the mold assembly;
c) Manufacturing the first half of the mold;
d) Manufacturing of the second half-mold;
e) Making a model of the anti-torque blade from composite materials reinforced with glass fibers, to check and adjust the molding process;
f) Fabrication of the coating on the surfaces of the two half molds;
g) Positioning the honeycomb core inside the mold and joining it with the shell;
h) Construction of the resistance spar from unidirectional carbon fibers;
i) Joining all the elements and closing the molds, in screws, for sealing;
j) Extraction of the composite blade from the mold after the polymerization time, followed by the external finishing.

The construction of the composite blade was a laborious manufacturing process, which involved an extensive set of practical knowledge needed to process composite materials. The purpose of the practical approach was to assemble, in a unitary composite material, the following main components, whose material characteristics were determined in the previous chapters:

- the skin - made of a laminated composite material reinforced with carbon fibers, consisting of three layers of carbon twill fabric 285 gr/m2, joined with epoxy resin; the composite blade cover encloses central elements and has a total thickness of approximately 1 mm;
- the spar - was made of unidirectional carbon fibers (roving), impregnated with epoxy resin, being arranged around the mounting bushings of the anti-torque blade, with longitudinal extension towards the free extremity.
- the honeycomb core - with hexagonal cells, made by thermoplastic extrusion.

In addition, two bushings with an inner diameter of 0.6 mm, made of a steel similar, in terms of mechanical characteristics, to that used for the actual blade were placed in the blade embedment area. These are mated to the blade spar and serve as an attachment point to the helicopter's rear rotor assembly.

The manufacturing process of the composite blade started by making a provisional model from malleable epoxy resin, based on the aerodynamic profile of the anti-torque blade. On this elongated airfoil, the two symmetrical half-matrices were built, having the separation plane at the chord level of the NACA0012 profile. The provisional model was made from the dimensions taken from the technical drawing of the anti-torque blade of the IAR330 helicopter, completed with local measurements from a real metal blade.

The two half molds made of sheet aluminum have bushings and guide areas as well as screw-tightening holes. When closing the half-molds, the screws will be progressively tightened

in opposite directions, to ensure a good tightness of the inner model. On the inner face of one of the half molds, two holes were made, on which the supports of the embedding bushings will be placed, at the time of the manufacture of the spar from carbon roving. The bushings will represent an integral part of the resistance spar, the unidirectional fibers being positioned around them, and their joining into a solid body being made with the help of epoxy resin.

The honeycomb core was made by thermoplastic extrusion, its fixation to the whole structure being ensured by adhesion with Derakane 470-300 epoxy resin. This component is made, in correspondence with the two half-matrices, also in the form of symmetrical half-planes with respect to the central-horizontal axis, being positioned inside the composite blade. The joining of the two half-matrices was realized at the central plane of the half-matrices.

Polymerization of the resin takes about 24 hours, being carried out at room temperature, after which the carbon fabrics that exceed the level of the molds are cut and adjusted.

The unidirectional carbon spar was made using a template, by placing it in the half-mold, over the laminated wax layer. The carbon roving wrapped around the steel bushings until the outer skin mold was filled with epoxy resin up to the dash. The same operations described previously were performed for the other half of the tail rotor blade. The resin and curing agent, applied over the unidirectional carbon, were carefully weighed and dosed to impregnate it.

The polymerisation time of the composite materials is 24 hours, during which the two half molds are tightened with clamping screws on the contour. A wooden structure was designed, which allows the uniform closing of the half-molds along their entire contour. The polymerization process is carried out under ambient conditions, at a temperature of approximately 23°C and with low air humidity.

After the polymerization time has passed, the composite blade is extracted from the inside of the two molds (fig. 7.1). Finishing the blade, in order to obtain the final shape, involved eliminating excess surfaces, cleaning the demoulding agent and applying a protective varnish.

Fig. 7.1 The final composite tail rotor blade at a scale of 1:3

7.2 Experimentally testing the composite blade by applying a bending force on the free edge

In order to experimentally verify the anti-torque blade made of composite materials on a scale of 1:3, it was decided to stress it by applying a vertical force positioned towards the free extremity. The objective of this type of test is to determine the behavior of the tail rotor blade, the experimental results will be used to validate the numerical analysis based on the same type of test.

This type of experimental test actually represents a simplified adaptation of the fatigue test of blades made of composite materials, according to the test methodology described by

specialized publications [30, 31, 32]. Such tests are based on devices equipped with one or more monoaxial or biaxial actuators (depending on the desired type of stress), which load and unload the blade during a predefined number of test cycles. Fatigue testing of blades made of composite materials in this way is the most frequently used option, both for blades in the aeronautical industry and for wind turbine blades.

Using the Instron 8872 as the measuring device, as well as for applying the imposed displacement, was the best solution from a practical point of view, due to the fact that the accuracy of the Instron force cell used in the blade testing is much higher compared to the other alternatives existing (micrometer, laser rangefinder, digital image correlation, etc.).

The composite blade was embedded by a strong enough aluminum beam to prevent it from buckling when the blade was loaded, which would result in erroneous results. The embedment was achieved by using two tightly tightened screws, positioned inside the metal bushings, so that the blade returns to its initial position when the movement stops, given the load from the elastic domain of the materials used (fig. 7.2).

Fig. 7.2 Positioning the composite blade inside the test rig

The metal support with a rectangular profile was later provided with a fixing screw at the end opposite the embedment area. By means of this screw, the support was fixed in the lower hydraulic tank of the Instron 8872 equipment, and in the upper hydraulic tank a metal element was fixed, by means of which the anti-torque blade will be required until a maximum displacement of 10 mm is reached.

In total, five experimental tryouts were carried out, in the previously presented configuration. A constant displacement of 2 mm/min was introduced into the equipment's interface software, with the equipment stopped by the operator when 10 mm of displacement was reached. The presented graph indicates a constant linear response for each individual case, the maximum force measured being in the range of 10.049÷12.092 N. The total duration of each test was approximately 300 seconds. During the tests, no residual deformation was observed, the blade always returning to its original position.

The previously specified data will be used to carry out the numerical analysis corresponding to this type of test, in order to validate the numerical model that will be used in carrying out future numerical simulations.

7.3 Comparative analysis of the blade performance according to the manufacturing material

The performance of the anti-torque blade made of composite materials was evaluated in the framework of static analyzes performed with the finite element program Ansys, in the context of using conditions similar to the numerical analyzes performed on the metal blade.

Given the practical difficulty, as well as the high level of danger associated with mounting the composite blade on a rotor capable of faithfully reproducing the specific characteristics of a hover flight or a forward flight, it was decided to verify the behavior under aerodynamic stresses by using a subsonic wind tunnel. Thus, in the previous chapters, the aerodynamic demands were determined using the Fluent module of the Ansys program and later, these values were validated based on the experimental results, to be used for a comparative analysis, in the case of the manufacture of the blade from aluminum alloys, respectively from composite materials.

The determination of the aerodynamic loading of the blade in order to introduce it into the structural static analysis was carried out by simulating the flow of the air current around the blade, within the Fluent module, being identical for both types of blade studied. The aerodynamic loads were determined for an air flow velocity of 50 m/s, linearly distributed along the length of the geometrically modeled blade at a scale of 1:1. All four reference values of blade incidence from the variation range specific to the antitorque rotor of the IAR330 helicopter ($+2.5^o \div -15.5^o$) were addressed.

The flow model used to determine the aerodynamic pressures is k-ε realizable, having the turbulent viscosity. It represents one of the most common and most complete options for performing the calculation of a turbulent flow, which uses transport equations to determine the kinetic energy of turbulence (denoted by "k") and their dissipation rate (denoted by "ε").

The skin of the 1:1 modeled blade is discretized with SHELL type elements, consisting of a total of nine sheets of carbon fiber fabric and epoxy resin. Modeling of the shell as a laminated composite was done within the ACP Pre module of the Ansys program.

Due to the stress mode of the blade, the orientation of the fibers at an angle of 0^o is important, because the material takes the stress due to the centrifugal force produced by the rotation of the blade at the speed of 1278 rpm, and the orientation of the fibers at 90^o is important, due to the frontal aerodynamic stresses of the air current. However, other factors, such as changing the incidence of the blade, the presence of uncontrolled wind gusts or vibrations during operation, cause the blade to be stressed in almost all directions, which is why it is necessary to have either the optimal arrangement of the blades in terms of their number, the sequence of overlap and fiber orientation, or choosing materials that provide good strength properties, regardless of the direction of blade loading/stress.

Also, given the identical nature of the stresses, the maximum displacement of the composite blade is located at its free end.

Experimental tests reveal a better breaking strength for two of the components of the composite blade, compared to the metal blade, thus being able to withstand higher intensity stresses. The breaking strength of the thermoplastic extruded honeycomb core is lower, but the composite blade as a whole compensates with the increased rigidity of the other two components, as well as with a greater thickness of the laminated composite skin (2.7 mm for the composite blade at 1:1 scale compared to 1 mm for the metal blade).

Increasing the angle of incidence leads to a directly proportional increase in the equivalent stress measured on the composite blade. Its main requested area is the foot of the blade, an integral part of the resistance spar, in the direction opposite to the air current, the material being compressed, as a result of the bending of the blade. At the shell level, the maximum stresses are predominantly found in the leading edge area, and in the case of the honeycomb core, the main stressed areas are the intersections of the hexagonal cell walls.

It can be seen how the increase of the maximum displacement is relatively constant, in the case of the maximum incidence allowed in operation $\alpha = 15.5^{o}$ it reaches a relatively high value. However, this is not a risk factor as the maximum equivalent stresses are relatively low compared to the breaking strength of each of the two more heavily stressed components: the unidirectional carbon spar and the laminated composite skin. Large values of the displacements can translate into a higher degree of elasticity of the composite blade.

Similarly to the maximum displacements, the specific deformations determined by the numerical analysis of the composite blade have higher values than in the case of the metal blade. Among the components of the composite blade, the maximum specific deformation is found in the case of the honeycomb core, in the area of the trailing edge, where the thickness of the NACA0012 profile narrows and the walls of the hexagonal cells have relatively small dimensions, acting similar to some tension concentrators.

The use of the constructive solution proposed by the present study, based on composite materials, led to the total reduction of the mass by approximately 41.54%. Broken down for each of the components, spar mass decreased by approximately 34.82%, honeycomb core mass decreased by approximately 56.70%, and shell mass decreased by 45.33%.

7.4 Conclusions

Following the experimental tests and numerical analyzes carried out on the anti-torque blade made of composite materials, the following important conclusions can be highlighted, which justify and support the idea of modernizing the tail rotor blader of the IAR330 helicopter, by transitioning to a composite configuration:

- **Fabrication cost** – according to the methodology presented in subchapter 7.1, the manufacturing process of the anti-torque blade by the manual method ("hand lay-up") offers the advantage of a low overall cost. Thus, the total value required for the manufacturing a composite tail rotor blade amounts to approximately 12000 lei, at the time of writing, while the value of a metal tail rotor blade, purchased through the certified supplier of parts for IAR330 helicopters, is approximately 25000 lei. The initial investment involves a higher cost, considering the fact that it is necessary to make additional molds on which the composite components will be placed. The manufacturing process can be significantly improved by introducing a vacuum pump for resin infusion, in order to obtain a standardized (series) final product.
- **Manufacturing complexity** – the manufacturing method of the composite blade described in this chapter involves significantly less complexity, being based, first of all, on the practical experience and theoretical knowledge of the workers, unlike the manufacturing process of the metal blade, which involves more equipment and devices special, as well as specialized/certified personnel in several fields.
- **Superior performances** – considering the experimental tests carried out by loading the free end of the blade, as well as due to the superior performance resulting from the comparative analysis of the composite blade and the metal blade, it can be concluded that this composite blade manufacturing configuration offers superior performance to the metal blade used currently. The performance of composite materials is characterized by high reliability, which, for the aeronautical industry, is an essential condition.
- **Switching to „on-condition" maintenance** – the implementation of composite materials in the structure of the tail rotor blade has the potential to allow the transition from a time dependent technical resource, established by the manufacturer, to an on-condition technical resource, given the higher reliability of this category of materials.

8. Final conclusions. Personal contributions and future perspectives

8.1 Considerations

The main objective of the doctoral thesis entitled "**Experimental and theoretical study of the transition towards a composite configuration for the IAR330 tail rotor blade**" was the provision of a practical alternative for the modernization of the tail rotor blade of the IAR330 helicopter, in the sense of the use of high-performance composite materials.

Choosing the advantageous constructive solution involved an extensive study regarding the variety of existing composite materials and how to manufacture them, in order to produce a reliable airworthiness component.

The research activity, carried out on both theoretical and practical foundations, required a complete set of interdisciplinary knowledge, such as: strength of materials, fluid mechanics, material science, digital image correlation, finite element method, etc. The experimental studies, carried out both locally, to determine the material properties, and globally, to evaluate the overall performances, served as the basis for validating the numerical simulations that prove the ability of the composite structure to perform under normal flight conditions.

8.2 Final conclusions

The doctoral thesis begins with a series of introductory theoretical information, intended to highlight the actuality of the doctoral thesis, as well as its importance, both from a scientific point of view and regarding the operation of the IAR330 helicopters, intended for the Romanian Air Force.

In chapter 1 - "The current stage of research" a synthesis was made of the main information available in the specialized literature, regarding the evolution of composite materials and specific aerospace applications, from which the following conclusions resulted:Fibrele de carbon și cele de sticlă sunt cel mai des întâlnite în componența structurilor aeronautice, datorită gradului ridicat de ranforsare. Fabricația unei structuri compozite ranforsate cu fibre de carbon permite atingerea unui nivel foarte ridicat de rezistență.

1. Epoxy resin is the heat-resistant polymer that ensures the best compatibility in use, together with carbon fibers, producing composite materials particularly resistant to stress.

2. The manufacture of blades from composite materials is a laborious process, based mainly on the practical experience of the manufacturer. In order to build a single prototype, the manual lamination method ("hand lay-up") is indicated.

3. The constructive solutions of composite blades identified during the research involve the use of a longitudinal spar, as the main resistance element, an inner core as light as possible, to minimize the total mass, as well as a shell made of layered composite material.

4. Additive manufacturing is a modern solution for prototyping and manufacturing quality components. Thermoplastic extrusion manufacturing represents the most accessible current solution for the construction of complex geometries.

In chapter 2 - "Objectives and organization of the thesis" the main general and specific objectives proposed to be achieved by this doctoral thesis were highlighted. The overall structure of the thesis was also presented, with a brief description of each individual chapter.

Chapter 3 - "Performance evaluations of the tail rotor blade of metallic construction" included the presentation of the main technical-tactical characteristics and the mode of operation of the helicopters. Taking as a reference the dimensions of the real blade and the main materials used by the manufacturer, the anti-torque blade was modeled, evaluating its performance in a numerical analysis carried out by the finite element method. Thus, the following conclusions could be drawn:

1. Among the multiple advantages of the transition to a composite structure, it is worth mentioning: the reduction of the total mass of the blade, thus increasing the total payload of the helicopter, the transition from a technical resource measured in time to a technical resource based on condition ("on-condition") , increasing the level of flight safety, as well as improving the overall resistance of the blade to external loads.

2. The numerical simulation of the flow was performed for a speed of 50 m/s, representing the maximum speed used in the wind tunnel, as well as for a speed of 206.5 m/s, representing the tangential speed at the tip of the blade during blade rotation, at the nominal speed of the anti-torque rotor.

3. The static analysis of the metal blade at the 1:1 scale allowed obtaining equivalent stresses and specific strains that will serve as a reference for evaluating the performance of the future composite blade.

4. The study of the two-dimensional aerodynamic flow around the blade profile, as well as the study of the fluid displacement around the three-dimensional model of the blade facilitated the visualization of the changes in the flow, corresponding to the change of the angle of incidence of the anti-torque blade.

The review of the main theoretical considerations related to the study of aerodynamic flow and the main flight regimes of the helicopter is presented in *chapter 4 - "Experimental validation of aerodynamic loads using the wind tunnel"*. The main conclusions that emerge from the study are:

1. Aerodynamic forces and their associated aerodynamic coefficients are the basis for conducting the study of fluid flow for any aeroelastic structure. Their variation depending on the incidence of the aerodynamic profile allows the identification of dangerous turbulent flow areas during flight.

2. The hover flight of the helicopter is the easiest to approach numerically, from the point of view of the external factors that can influence the condition of the tail rotor blade.

3. The subsonic wind tunnel, through its dimensional and speed characteristics, satisfies the similarity conditions necessary to validate the numerical analysis carried out in the Fluent module.

4. From the comparative analysis of the results determined experimentally in relation to the results of the numerical analysis, similar values emerged for the points on the blade cover, set as a reference.

Chapter 5 - "Determination of the mechanical and elastic characteristics of the materials that make up the composite anti-torque blade" includes the most extensive set of experimental data, obtained from traction, compression and bending tests, carried out with the aim of determining the mechanical characteristics of the materials that make up the composite anti-torque blade . The following important conclusions can be drawn:

1. The tensile tests performed on the unilaminar material, using the micro-DIC configuration, facilitate the observation of the behavior of the fibers and the matrix under the action of external stresses at a microscopic level, the results being closely related to those of the tensile behavior of the multilayer composite material.

2. From the comparative analysis of the compressive stress of the thermoplastic extruded honeycomb, in relation to the aluminum honeycomb, a higher strength of the aluminum alloy resulted, the thermoplastic extruded material compensating, on the other hand, through a lower mass, cost reduced manufacturing cost and corrosion resistance.

3. The variation of the material characteristics depending on the manufacturing direction led to the need to evaluate the orthotropic character of the thermoplastic extruded material, thus determining the optimal manufacturing direction of the honeycomb core, which would allow a maximum bearing capacity.

4. The complete set of experimentally determined mechanical characteristics allows a more faithful definition of the numerical model of the composite blade, in order to validate the numerical analyzes carried out with the finite element method.

In *chapter 6 - "Finite element modeling and analysis of mechanical tests of composite materials"*, a series of numerical analyzes was carried out aimed at verifying the correlation of the results of finite element simulations with the results obtained experimentally. Identified results show the following aspects:

1. By approaching each type of experimental test separately (tension, compression, bending), a preliminary validation of the mechanical behavior of the studied composite materials was carried out, the results being satisfactory in terms of the determined error.

Chapter 7 - "Manufacturing and experimental testing of the tail rotor blade from composite materials. Validation of specific numerical analyses" presents the main steps taken for the practical realization of the tail rotor blade and its testing, so that a comparative analysis can be carried out in relation to the real blade. The main aspects that can be concluded are:

1. The manufacture of the blade was a labourious process, based on numerous practical technical knowledge. The manufacturing process was specially adapted to obtain the composite blade prototype at 1:3 scale, requiring multiple manufacturing accessories, made especially for this purpose (moulds, models for adjustment, etc.)

2. From the comparative analysis of the numerical simulations performed for the anti-torque blade in the metallic version, as well as in the version made of composite materials, it emerged that the replacement of aluminum alloys with the proposed composite materials offers increased resistance to aerodynamic stresses.

3. Compared to the metal blade, the manufacturing process of the composite blade involves a lower level of complexity, with less special equipment and devices involved.

4. The experimental test of applying an eccentric force in the vertical plane, on the free extremity, represented the final test that validated the numerical model of the composite blade, which can be used in future numerical simulations for performance evaluation.

8.3 Personal contributions and future perspectives

The doctoral thesis had as its main objective the experimental determination of a viable constructive solution, made of composite materials, to modernize the anti-torque blade of the helicopter, increasing the degree of reliability, as well as the level of flight safety.

Through the scientific research activity carried out, both at a theoretical and at a practical level, the following *personal contributions* can be deduced, regarding the increase in the performance of the tail rotor blade of the IAR330 helicopter:

a) Carrying out a bibliographic study regarding the composite materials used in the construction of helicopter blades, from the perspective of nature, manufacturing method and general physical properties, in order to investigate the compatibility between the constituent elements of the composite materials used in the blade.

b) Synthesizing the main manufacturing methods of composite materials, as well as the constructive solutions identified for similar composite blades in operation.

c) Numerical analysis (CFD) of two-dimensional and three-dimensional type for the study of the aerodynamic flow around the anti-torque anti-torque blade, positioned at different incidences from the practical operating orientation range (2.5°÷-15.5°), as well as for different air speeds.

d) The use of the wind tunnel to validate the pressures obtained through numerical analyses, on a geometric model of the blade made on a real scale and specially processed to allow the installation of pressure measurement accessories on the outer surface of the shell.

e) The study of the orthotropic character of the thermoplastic extruded material, in order to determine the optimal orientation for taking over the aerodynamic loads.

f) Carrying out a comparative analysis regarding the tensile test of a laminated composite material made of carbon fiber fabric and epoxy resin, to correlate the effects observed at the microscopic level (unilaminar material) and at the macroscopic level (multilaminar material).

g) Realization of a hybrid structure from the point of view of the manufacturing technique, containing laminated composite materials and materials made by additive manufacturing.

h) Establishing the advantageous constructive solution for manufacturing the composite blade, keeping the external geometric characteristics of the initial anti-torque blade.

i) Realization of a methodology for the manufacture of composite blades by the "hand lay-up" method, which can be reused for the manufacture of future blades.

j) Fabrication of the 1:3 scale composite blade and its experimental testing by applying a force to the free end, using the force cell of the INSTRON equipment and an embedment device specially designed for this purpose.

k) Carrying out a comparative analysis of honeycomb structures with hexagonal cells, made of chlorinated polyethylene filament reinforced with carbon microfibers, on the one hand, and of aluminum alloy 5052 type NIDA, on the other.

Considering the current achievements of this doctoral thesis, the following *research perspectives* can be highlighted, in order to deepen the current theme and to establish the airworthiness of the composite blade:

a) Carrying out the necessary numerical analyzes for the faithful simulation of the flight conditions encountered in the hover flight regime, as well as in the forward flight regime.

b) The integration of high-precision polymer sensors into the structure of the composite blade, in order to monitor the state of structural integrity of the blade and for the immediate identification of damage suffered during operation.

c) Improving the manufacturing process by using a vacuum pump to uniformly infuse the resin into the internal structure of the composite blade.

d) Extending the methodology for testing the composite blade, by applying the eccentric force in order to study the fatigue resistance.

e) Passing through the stages required by the specific regulations of the National Military Aeronautical Authority (A.A.M.N.), in order to obtain the quality certification for the cataloging of the anti-torque blade made of composite materials as an aeronautical product.

BIBLIOGRAPHY

[1] Timoshenko, S. P., *History of Strenght of Materials*, Dover Publications Inc., New Tork, 2019, ISBN-13: 978-0-486-61187-7.

[2] https://www.owenscorning.com, accesat la data de 14.05.2022 ora 18.30.

[3] https://www.ge.com/additive/additive-manufacturing/industries/aviation-aerospace, accesat la data de 16.05.2022 ora 14.20.

[4] https://www.airbus.com/newsroom/news/en/2017/02/Material-evolution.html, accesat la data de 16.05.2022 ora 18.00.

[5] Federal Aviation Administration - AMT Airframe Handbook Volume 1 (FAA-H-8083-31), ISBN-13: 978-1548241834.

[6] Ghobadi, A., *Common Type of Damages in Composites and Their Inspections*, World Journal of Mechanics, 2017, vol. 07, pag. 24-33.

[7] http://www.appropedia.org/Composites_in_the_Aircraft_Industry, accesat la data de 17.05.2022 ora 10.00.

[8] Hadăr, A., *Structuri din compozite stratificate*, Editura Academiei şi Editura AGIR, Bucureşti, 2002, ISBN 973-27-0961-8 şi ISBN 973-8466-25-3

[9] Baker, A. A., Scott, M., Composite Materials for Aircraft Structures, AIAA - American Institute of Aeronautics, ISBN: 9781624103261.

[10] Gunkler, A., Archibald, M. C., *Composite Propeller Construction*, 2011 ASEE NC & IL/IN Section Conference, 2011.

[11] Hou, W., Zhang, W., *Advanced Composite Materials defects/damages and health monitoring*, Proceedings of the IEEE 2012 Prognostics and System Health Management Conference (PHM-2012 Beijing), pp. 1-5, Beijing, 2012.

[12] Amafabia, D. M., Montalvão, D., David-West, O., Haritos, G., *A Review of Structural Health Monitoring Techniques as Applied to Composite Structures*, Structural Durability & Health Monitoring Journal, vol. 11(2), 2017.

[13] https://en.wikipedia.org/wiki/Spar_(aeronautics), accesat la data de 26.05.2022 ora 14.00.

[14] Kovalovs A., Barkanov E., Ruchevskis S., Wesolowski M., *Optimisation Methodology of a Full-Scale Active Twist Rotor Blade*, 16th Conference on Reliability and Statistics in Transportation and Communication, RelStat'2016, Riga, Latvia, 19-22 October, 2016.

[15] Rasuo B., Full-Scale Fatigue Testing of the Helicopter Blades from Composite Laminated Materials in the Development Process, Journal of the Mechanical Behavior of Materials, 19(5), October 2009.

[16] Pflumm, T., Rex, W., Willem RexManfred HajekManfred Hajek, Propagation of Material and Manufacturing Uncertainties in Composite Helicopter Rotor Blades, 45th European Rotorcraft ForumAt: Warsaw, September 2019

[17] Miller M., Narkiewicz J., Kania W., Czechyra T., The application of helicopter rotor blade active control systems for noise and vibration reduction and performance, Materials Science, 2006.

[18] ISO/ASTM 52900:2015, Additive manufacturing - General principles – Terminology.

[19] **Voicu, A.-D.**, Hadăr, A., Vlăsceanu, D., *Benefits of 3D printing technologies for aerospace lattice structures*, Scientific Bulletin of Naval Academy, Vol. XXIV 2021, pg.8-16, ISSN: 2392-8956, dată publicare: 22.07.2021, doi: 10.21279/1454-864X-21-I1-001.

[20] Manualul de zbor al elicopterului IAR330 emis de Societatea IAR S.A. Braşov.

[21] Baker, C., Johnson, T., Flynn, D., Hemida, H., Quinn, A., Soper, D., Sterling, M., *Train Aerodynamics*, ISBN 9780128133101, 2019.

[22] http://nptel.ac.in/courses/Webcourse-contents/IIScBANG/Composite%20Materials/pdf /Lecture_Notes/LNm1.pdf, accesat la data de 30.06.2022 ora 15.00.

[23] https://www.flight-mechanic.com/helicopter-flight-conditions-part-one/, accesat la data de 10 februarie 2022.

[24] Bramwell, A.R.S., *Helicopter Dynamics*, Edward Arnold Ltd., London, 1976.

[25] G. K. Batchelor, *An Introduction to Fluid Dynamics*, Cambridge University Press, June 2012, ISBN: 9780511800955.

[26] Aydın, N., Çalışkan, M.E., Karagoz, I., *Numerical Simulation of Flow Over Different Types of Airfoils*, 8th International Conference on Advanced Technologies, ICAT 2019.

[27] ASTM D3039, Standard Test Method for Tensile Properties of Polymer Matrix Composite Materials.

[28] ASTM C365, Standard Test Method for Flatwise Compressive Properties of Sandwich Cores.

[29] ASTM D790, Standard Test Methods for Flexural Properties of Unreinforced and Reinforced Plastics and Electrical Insulating Materials.

[30] Fișă date tehnice oferită de producătorul Fillamentum Industrial pentru filamentul CPE CF112 Carbon.

[31] Fișă date tehnice oferită de producătorul Torayca Carbon Fibers America Inc. pentru materialul T300.

[32] Fișă date tehnice oferită de producătorul Derakane pentru rășina epoxidică Momentum 470-300.

[33] Fișă date tehnice oferită de producătorul Castro Composites pentru țesătura GG285T.

[34] Hadăr, A., Baciu, F., **Voicu, A.-D**., Vlăsceanu, D., Tudose, D. I., Adetu, C., *Mechanical Characteristics Evaluation of A Single Ply and Multi-Ply Carbon Fiber-Reinforced Plastic Subjected to Tensile and Bending Loads*, Polymers 2022, 14, 3213, ISSN 2073-4360, https://doi.org/10.3390/polym14153213, Factor de impact - 4.967, clasificare Scopus - Q1 pe domeniul "Polymer Science".

[35] **Voicu, A.-D.**, Hadăr, A., Vlăsceanu, D., *Aspects regarding interlaminar stress distribution on the composite laminated skin of a tail rotor blade exposed to aerodynamic forces*, Vol. 12, no. 1, 2020, Annals Series on Engineering Sciences, ISSN: 2066-8570.

[36] **Voicu, A.-D**., Hadăr, A., Vlăsceanu, D., Improving the Mechanical Behavior of a Helicopter Tail Rotor Blade Through the Use of Polyurethane Foams, Revista de Chimie (Rev. Chim.), Year 2019, Volume 70, Issue 11, 4123-4127, dată publicare: 15.12.2019, ISSN: 2668-8212, https://doi.org/10.37358/RC.70.19.11.7716.

[37] **Voicu, A.-D**., Hadăr, A., Vlăsceanu, D., Tudose, D. I., Vibrational Study of a Helicopter Tail Rotor Blade with Different Polymer Inner Core Materials, Materiale Plastice (Mater. Plast.), Year 2020, Volume 57, Issue 2, 169-178, dată publicare: 01.07.2019, ISSN: 2668-8220, https://doi.org/10.37358/MP.20.2.5363.

[38] **Voicu, A.-D.**, Hadăr, A., Pastramă, Ș, Vlăsceanu, D., *SHM Monitoring Methods and Sensors with Applications to Composite Helicopter Blades: A Review*, Acta Universitatis Cibiniensis. Technical Series, Sciendo, 2020, dată publicare: 01.12.2020, ISSN: 1583-7149.